water

MDPI

Article

Performance Enhancement of Specific Adsorbents for Hardness Reduction of Drinking Water and Groundwater

Parnian Ghanbarizadeh [1], Mohammad Mehdi Parivazh [2], Mohsen Abbasi [1,*], Shahriar Osfouri [1], Mohammad Javad Dianat [1], Amir Rostami [1], Mahdieh Dibaj [3] and Mohammad Akrami [3,*]

[1] Department of Chemical Engineering, Faculty of Petroleum, Gas and Petrochemical Engineering, Persian Gulf University, Bushehr 75169-13798, Iran
[2] Department of Chemical Engineering, Amirkabir University of Technology (Tehran Polytechnic), Tehran P.O. Box 15875-4413, Iran
[3] Department of Engineering, University of Exeter, Exeter EX4 4QF, UK
* Correspondence: m.abbasi@pgu.ac.ir (M.A.); m.akrami@exeter.ac.uk (M.A.)

Abstract: One of the most advantageous methods for lowering water hardness is the use of low-cost adsorbents. In this research, the effectiveness of natural zeolite (clinoptilolite type), activated carbon, and activated alumina was evaluated. These adsorbents were sequentially modified by NaCl, HCl, and NaCl-HCL to improve their ability to adsorb. The contact time and the amount of adsorbent used in the adsorption process were investigated experimentally to determine their effects. The results indicated that the best contact time for hardness reduction was 90 min, and the best concentrations of adsorbents in drinking water for zeolite, activated carbon, and activated alumina were 40, 60, and 60 g/L, respectively. In addition, for groundwater, these figures were 60, 40, and 40 g/L, respectively. The greatest possible decreases in total hardness under the best conditions by natural zeolite, activated carbon, and activated alumina adsorbents were 93.07%, 30.76%, and 56.92%, respectively, for drinking water and 59.23%, 15.67 %, and 39.72% for groundwater. According to the results obtained from experiments, NaCl-modified zeolite, natural zeolite, and NaCl-HCl-modified activated carbon performed better in terms of parameter reduction. The equilibrium data were well fitted by the Langmuir isotherm model, whereas the kinetic data for the adsorption process were consistent with the pseudo-second-order model. The equilibrium study of the adsorption process by the Morris–Weber model revealed that both chemical and physical adsorption are involved.

Keywords: zeolite; activated carbon; activated alumina; hardness; adsorbent modification

Citation: Ghanbarizadeh, P.; Parivazh, M.M.; Abbasi, M.; Osfouri, S.; Dianat, M.J.; Rostami, A.; Dibaj, M.; Akrami, M. Performance Enhancement of Specific Adsorbents for Hardness Reduction of Drinking Water and Groundwater. *Water* **2022**, *14*, 2749. https://doi.org/10.3390/w14172749

Academic Editors: Imran Ali, Juying Li, Changsheng Peng and Iffat Naz

Received: 3 August 2022
Accepted: 1 September 2022
Published: 3 September 2022

1. Introduction

Groundwater is one of the main drinking water sources in areas with growing populations. In many countries, about 60% of drinking water and 30% of water for agriculture come from groundwater [1]. Water pollution has become one of the most pressing issues and can be the main cause of diseases and mortality all over the world. Three types of pollutants in water are organic matter, minerals, and physical factors [2]. Mineral contaminants can cause water turbidity and, in some cases, appear as suspended particles in water. Moreover, water pollutants include mineral salts such as calcium and magnesium, inorganic acids, and metal compounds that cause the acidity and toxicity of water [3].

Corrosion and sedimentation are important indicators of water quality assessment [4]. The sedimentation process involves the combination of divalent metal ions with hardness factors in water [5]. Water hardness is caused by some multivalent metal ions, such as calcium (Ca^{2+}) and magnesium (Mg^{2+}). Excessive intake of calcium and magnesium can lead to osteoporosis, kidney stones, colon cancer, high blood pressure, etc. [6]. World Health Organization (WHO) guidelines recommend drinking-water-permissive levels of 40–80 ppm calcium and 20–30 ppm magnesium. In addition, the total hardness, which is the concentration of both calcium and magnesium, is between 2 and 4 mmol/L [7].

Sedimentation of some water-soluble solids in pipes and tanks reduces the water flow rate and heat transfer, increases the pressure drop and energy use in water pumping, clogs pipes, and raises the costs of the operation and maintenance of water supply systems. If the above deposits are not controlled, they will increase costs for water supply systems [8,9].

Various methods have been proposed to reduce the hardness of water. The main ways of separating ions in water are thermal methods, membranes, adsorption, magnetic methods, and ion exchange [7]. Thermal methods are not economical due to their high energy consumption and low efficiency. In membrane methods, biological clogging, membrane degradation, and, in the case of reverse osmosis, high osmotic pressure, high energy consumption, and outlet water balance of reverse osmosis in terms of solutes can be mentioned [10,11]. Magnetic methods are not industrialized because they are not highly reliable [12]. Ion exchange methods are widely employed to remove ions due to their advantages, including high capacity, very high efficiency, and high speed [13]. The use of ion exchange resins is also expensive. The adsorption process is superior to other methods due to its low cost, ease of operation, and simplicity of design [14]. Various adsorbents have been used to remove various ions from wastewater in several lab-scale studies, such as activated alumina, activated carbon (AC), biomass, clay, industrial waste from coal, and zeolite. High-carbon adsorbents effectively remove organic and inorganic contaminants, while high-mineral adsorbents are effective only in removing mineral contaminants, especially metal [15]. Clinoptilolite, the most common of the 40 types of natural zeolites, is an attractive choice for water and wastewater treatment because of its low price and large surface area [16]. The general mechanism of zeolite is ion exchange; this capability allows zeolite to exchange and adsorb cations in water [17]. The price of each kilogram of zeolite is reported to be USD 0.08 [18]. One of the most desirable properties of AC is its high levels of thermal, mechanical, and light stability. Other features include its porous and solid structure, high surface-to-volume ratio, and high purity [19]. The price of each kilogram of activated carbon is reported to be USD 2.2 [18]. Alumina is one of the most widely used ceramic materials and is called a series of irreversible forms of hydroxyl aluminum oxide. These are porous solids obtained by heating aluminum hydroxides [20].

Many researchers have tried to remove hardness ions from drinking water by thermal, membrane, adsorption, ion exchange resins, and magnetic methods [21–30]. Among these methods, adsorption is a simple, effective, and inexpensive method. Adsorption can be employed as pre-treatment. Mubarak et al. [31] studied the adsorption of heavy metals and hardness ions in groundwater on TiO_2-supported zeolite-4A in both continuous and batch modes. The optimal pH range for Fe (III) and Mn (II) recovery using zeolite composites was determined to be 6–8. The findings suggested that the modified adsorbent has good removal effectiveness. Kaewmee et al. [32] used a batch adsorption process to reduce water hardness by a Geopolymer cube adsorbent activated with potassium derived from waste coal fly ash. It was shown that Ca^{2+} and Mg^{2+} had maximum adsorption capacities of 52.0 and 17.3 mg/g. Rolence et al. [25] investigated hardness removal using activated carbon produced from coconut shell. The results showed that pH 6.3 had the highest hardness removal value of 55%. The best adsorbent amount was 24 g/L. Although more removal was observed at pH = 12, it was not economical due to the need for more pH modifiers, and it led to the entry of chemical pollutants into the soft water. Cai et al. [33] investigated the synergy between cobalt and nickel on $NiCo_2O_4$ nanosheets that promotes peroxymonosulfate activation for efficient degradation of norfloxacin. Zhang et al. [34] studied the in situ synthesis of FeS/carbon fibers for the effective removal of Cr(VI) in aqueous solutions. The results showed the removal of 81.62% mg/g of chromium (VI). Pourshadlou et al. [35] investigated the adsorption of Mg^{2+} using bentonite/γ-alumina nanocomposites. A number of process variables, such as the amount of alumina, the starting ion concentration, the dose of adsorbent, the length of contact, and pH, were studied in relation to Total Organic Carbon (TOC). The quantity of adsorbed magnesium ions per gram of adsorbent decreased when the alumina content of the composite was enhanced from 1% to 3% and 5% by weight. The adsorption capacity of biochar prepared using banana peels

and wheat straw by the pyrolysis process was investigated by Gabol et al. [36] to remove Chemical Oxygen Demand (COD) and Total Dissolved Solids (TDS) from wastewater. Adsorption efficiency was maximized at a dose of 1 g for 50 mL of the component. Wheat straw and banana peel biochar reduced COD levels from 1985 to 973 mg/L and 1021 mg/L, respectively. TDS levels also dropped significantly. Farrag et al. [21] investigated the removal of hard salts from groundwater by thermogenic zeolite. Total hardness decreased by 35% to 100%. Zuo et al. [37] examined the elimination of COD with a simple method for modifying activated carbon fibers using the calcination method. An acid-to-base conversion of surface functional groups was seen, removing some of the ions in activated carbon fibers. Kumari et al. [38] investigated fluoride removal from industrial effluents using sulfuric acid-modified alumina. Acid modification raised the active surface area of alumina, and the results showed that after modification, fluoride removal increased from 63.5% to 96.72%. Activated alumina was found to have a good potential for fluoride removal from effluents but was less prone to use relative to its price. Zereffa et al. [39] studied the removal of hardness ions, nitrite, and iron using a ceramic filter prepared with soft wood and kaolin. The results showed that calcium, magnesium, iron, and nitrite removal were 63.08%, 54.3%, 72.77%, and 70.56%, respectively.

In studies by other researchers, modifiers such as KNO_3, surfactant, $CaCl_2$, and NH_4Cl were used to modify the zeolite adsorbent. Sulfuric acid, hydrochloric acid, and sodium chloride were also used separately to remove cadmium and arsenic. Sulfuric acid was also used to modify the alumina adsorbent to remove fluoride. The novelty of this study is the use of adsorbents of zeolite, activated carbon, alumina, and their modified forms to remove the hardness of drinking water and groundwater. These adsorbents were modified using HCl and NaCl separately and sequentially. In fact, the sequential modification of the adsorbents is the distinguishing feature of this research. Kinetic and isotherm investigations were also conducted under optimum conditions, and the reaction sequence and proper isotherm model were determined based on the best fit.

2. Materials and Methods

2.1. Adsorbents and Materials

In this study, different adsorbents were used to reduce the hardness of drinking water and groundwater. The adsorbents and their physicochemical properties (Table 1) are summarized. The natural zeolite clinoptilolite type was purchased from Afrazand Co., Tehran, Iran. Activated alumina and activated carbon were provided by the Iranian Institute of Research & Development in Chemical Industries, Karaj, Iran, and Shimi Pajoohan Co., Tehran, Iran, respectively.

To pre-prepare zeolite and activated carbon as adsorbents, first, the crushed adsorbents were sieved by 7-mesh ASTM standard sieves (2.8 mm). Then, the adsorbents were washed several times with abundant distilled water so that the TDS values of the aqueous solution and adsorbent were nearly the same as the TDS value of distilled water. The adsorbents were then dried in an oven at 55 °C for 24 h. The activated alumina adsorbent, which was in the form of granules, only underwent the washing and drying steps, as already mentioned for the pre-preparation.

An ammonia buffer solution containing 32% ammonia solution, ammonium chloride with a purity of 99.8%, magnesium sulfate with a purity of 99.5%, and EDTA with a purity of 99.8% was used in the experiment to determine the hardness of the water by complexometric titration. Sodium hydroxide with a purity of 99.5% and Eriochrome Black T reagent (with the chemical formula $C_{20}H_{12}N_3O_7SNa$) with a purity of 99.8% were used in hardness titration. In addition, the reagents Murexide or Ammonium Purate ($NH_4C_8H_4N_5O_6$ or $C_8H_5N_5O_6NH_3$) with a purity of 99.5% for use in complexometry titration, especially for calcium ions (water hardness agent), Ethylenediaminetetraacetic acid (EDTA) with a purity of 99.8%, and 37% concentrated hydrochloric acid (HCl) were used. All chemical materials were provided by the German company Merck.

Table 1. Characteristics of natural zeolite clinoptilolite and activated alumina.

	Composition	Content (wt.%)
Zeolite	SiO_2	68.5%
	Al_2O_3	11%
	Na_2O	3.8%
	K_2O	4.4%
	CaO	0.6%
	Fe_2O_3	0.2%
	Loss on ignition (L.O.I)	11.5%
Activated alumina	Al_2O_3	6%
	L.O.I	6%
	Na_2O	0.35%
	Fe_2O_3	0.02%
	SiO_2	0.02%

2.2. Characterization of Adsorbents

In order to precisely characterize the surface morphology, structure, and cavities of the adsorbents, they were subjected to scanning electron microscopy (SEM, TESCAN, Brno, Czech Republic), X-ray diffraction (XRD, Philips, Amsterdam, The Netherlands), and Brunauer–Emmett–Teller (BET, Micromeritics Corporate Headquarters, Norcross, GA, USA).

2.3. Water Samples

Drinking water from Bushehr city, Iran, and groundwater (prepared from domestic well water of the old structure of Bushehr city, Iran) were used in this study. Table 2 lists the analysis results of drinking water and groundwater.

Table 2. Drinking water and groundwater sample analysis.

	Parameters	Unit	Values
Drinking water	Total hardness	(mg/L $CaCO_3$)	520
	TDS	(mg/L)	627
	EC	(µS/cm)	1248
	Calcium	(mg/L)	166.73
	Magnesium	(mg/L)	25.27
	pH	-	7.72
Groundwater	Total hardness	(mg/L $CaCO_3$)	1148
	TDS	(mg/L)	1330
	EC	(µS/cm)	2361
	Calcium	(mg/L)	218.03
	Magnesium	(mg/L)	146.77
	pH	-	7.82

2.4. Adsorption Experiments

In this research, the experiments were conducted in two stages. First, the performance of each adsorbent was evaluated separately, and parameters such as total hardness, Mg hardness, and Ca hardness determined by the titration method were calculated for each one.

All adsorption experiments were carried out in batch mode. Initially, different amounts of the above adsorbents (1.2, 2.4, 3.6, and 4.8 g) were weighed separately. Then, these adsorbents were added to a 250 mL Erlenmeyer flask containing 60 mL of the drinking water sample. The concentrations of these adsorbents were 20, 40, 60, and 80 g/L. In each experiment, each concentration was poured into six conical flasks and placed on a shaker with a constant rotation speed of 150 rpm. Each time the contact time elapsed (10, 20, 30, 60, 90, and 120 min) and the adsorption test was performed, one of the samples was taken from the shaker. Next, the solution was filtered by passing it through Whatman filter paper, Grade 42, Germany, and the samples were prepared for analysis. These tests were repeated for groundwater samples. Second, after determining the optimum concentration of each adsorbent, a modification test was performed at that concentration. First, the best concentration (gr) of adsorbent was added to six conical flasks containing 50 mL of the modifier. The samples remained in the modifier for 24 h. The conical flask containing the adsorbent and modifier was then placed on a shaker at a constant rotational speed of 150 rpm for 1 h at room temperature. After passing the solution through a filter paper, it was washed several times with distilled water to achieve neutral pH. The TDS value should also be almost the same as the TDS value of the distilled water. It was then placed in the oven at 55 °C for 24 h to dry. Hardness was assessed after repeating these procedures on samples of groundwater. Adsorbents that were used up were gathered and put in containers with labels and a tight seal.

The removal of hardness ions (calcium and magnesium) in each experiment was determined using the following equation:

$$\text{Removal Efficiency} = \frac{C_i - C_f}{C_i} \times 100 \quad (1)$$

C_i and C_f (mg/L) are the initial and final concentrations of ions (calcium and magnesium) in the solution, respectively.

To calculate the amount of ions (calcium and magnesium) adsorbed by the adsorbent in time t, the following equation can be used:

$$q_t = (C_i - C_t) \times \frac{V}{m} \quad (2)$$

q_t (mg/g) is the amount of ions (calcium and magnesium) adsorbed per unit mass of adsorbent at time t, C_t (mg/L) is the concentration of ions (calcium and magnesium) in solution at time t, V (L) is the solution volume, and m (g) is the adsorbent mass.

In addition, to calculate the adsorption capacity at equilibrium, the same equation can be used:

$$q_e = (C_i - C_e) \times \frac{V}{m} \quad (3)$$

q_e (mg/L) is the amount of ions (calcium and magnesium) adsorbed per unit mass of adsorbent at equilibrium, and C_e (mg/L) is the concentration (calcium and magnesium) in solution at equilibrium.

2.5. Measurement of Target Parameters

2.5.1. Measurement of Total Hardness

First, 25 mL of water was poured into a conical flask. Then, ammonium buffer (1 mL) was added to keep the pH constant. A few drops of Eriochrome Black T reagent were then added to this solution. When Eriochrome Black T is added, it forms a red complex with calcium and magnesium cations at a pH of about 10. This complex is broken down by the addition of EDTA, releasing Eriochrome Black T and turning the sample blue. This stage

indicates the end of the titration. Equation (4) was used to calculate the total hardness in terms of calcium carbonate [40].

$$\text{Total hardness } (\text{mg/L}) = \frac{V_C \times f_c \times 10000}{V} \quad (4)$$

In the above relation, V_C (mL) is the volume of EDTA consumption, f_c is EDTA molarity, and V (mL) is the sample volume.

2.5.2. Measurement of the Calcium Hardness

The sample (25 mL) was poured into a 250 mL conical flask using a graduated pipette, and then 1 to 2 drops of NaOH 1 N and murexide reagent were added until the sample turned pink. Titration was then continued with 1 M EDTA standard solution until a purple color was formed. The volume of titrant consumed was recorded, and the calcium hardness was determined using Equation (5) [40]. Equation (6) was also used to obtain the concentration of calcium ions.

$$\text{Calcium hardness } (\text{mg/L}) = \frac{V_C \times f_c \times 10000}{V} \quad (5)$$

$$Ca^{2+}\left(\frac{mg}{L}\right) = \text{ Calcium hardness as} \frac{mg}{L} CaCO_3 \times 0.4004 \quad (6)$$

2.5.3. Measurement of Magnesium Hardness

Magnesium hardness was determined by subtracting the total hardness and calcium hardness according to Equation (7). Equation (8) was also utilized to calculate the concentration of magnesium ions [40].

$$\text{Magnesium hardness (mg/L)} = \text{Total hardness} - \text{Calcium hardness} \quad (7)$$

$$Mg^{2+}\left(\frac{mg}{L}\right) = (\text{Total hardness} - \text{ Calcium hardness}) \times 0.243 \quad (8)$$

2.6. Adsorption Isotherms

Adsorption isotherms were recorded using equilibrium data. These data are the most important information to describe and understand the adsorption process. Adsorption isotherms show the relationship between the concentration of ions present in the solution and the amount of ions adsorbed by the adsorbent at a constant temperature. The most widely used isothermal models to study the structure and operation of the adsorption process are the Langmuir and Freundlich isothermal models [41]. The linear form of these models is expressed in Equations (9) and (11). The Temkin isotherm model (Equation (13)) was studied to determine the adsorption energy and to obtain more information about the adsorption mechanism [42].

$$\frac{C_e}{q_e} = \frac{1}{q_{max} K_l} + \frac{1}{q_{max}} C_e \quad (9)$$

In this equation, q_e (mg/g) is the amount of adsorbate per unit mass of adsorbent at equilibrium, C_e (mg/L) is the equilibrium concentration, q_{max} (mg/g) is the maximum amount of adsorbate per adsorbent, and K_L (L/mg) is the Langmuir constant.

The separation factor R_L is another parameter that can assess the adsorption favorability. It is a crucial parameter in the Langmuir isotherm model, where $R_L > 1$ is an undesirable process, $R_L = 1$ is a linear process, $0 < RL < 1$ is a desirable process, and $R_L = 0$ is an irreversible process, which is expressed as follows:

$$R_L = \frac{1}{1 + K_L C_i} \quad (10)$$

where C_i (mg/g) is the smallest initial solution concentration.

$$\log q_e = \log K_F + \frac{1}{n} \log C_e \quad (11)$$

In this equation, K_F (mg/g) and (1/n) are the constants of the equation, in which K_F depends on the adsorption capacity, and 1/n indicates the adsorption intensity.

$$q_e = B \ln K_T + B \ln C_e \quad (12)$$

In this equation, B and K_T are Temkin constants. k_T (J/mol) is the change in adsorption energy between two adjacent adsorption sites.

2.7. Adsorption Kinetics

2.7.1. Diffusion-Controlled Adsorption Models

In general, distinguishing between adsorption processes controlled by intraparticle diffusion and those controlled by chemical reactions is difficult. One way to determine whether the process is controlled by intraparticle diffusion is to use the equation proposed by Morris and Weber [43]. This model is expressed in Equation (13).

$$q_t = K_{id} t^{0.5} + C \quad (13)$$

In this equation, q_t (mg/g) is the adsorption capacity at time t (h), K_{id} (g/mg.h) is the rate constant of adsorption capacity, and C (mg/g) is a constant representing the thick of film or diffusion resistance.

2.7.2. Chemical Reaction-Controlled Adsorption Models

The pseudo-first- and pseudo-second-order kinetic models are the types in which the adsorption process is controlled by a chemical reaction. Both of these equations are frequently used together in various studies, one of which is more consistent with the experimental information. The pseudo-first-order equation is as follows [44,45].

$$\log(q_e - q_t) = \log q_e - \frac{K_1 t}{2.303} \quad (14)$$

In this equation, q_t (mg/g) is the adsorption capacity at time t (h), and K_1 (h^{-1}) is the rate constant of the pseudo-first-order adsorption.

The pseudo-second-order equation is defined based on the equilibrium capacity, assuming that the degree of filling of adsorbent sites is proportional to the square of the number of empty adsorbent sites. The pseudo-second-order equation is expressed by the following [46].

$$\frac{1}{q_e - q_t} = K_2 t + \frac{1}{q_e} \quad (15)$$

where k_2 (g/mg.h) is the rate constant of the pseudo-second-order model.

3. Results and Discussion

3.1. Characterization of Zeolite, Alumina, and Activated Carbon

3.1.1. XRD

The XRD pattern shown in Figure 1a demonstrates the crystalline and structural properties of natural zeolite. C, Q, F, and M denote the four distinct phases of clinoptilolite, quartz, feldspars, and mordenite, respectively, that can be found in natural zeolite and are associated with peaks observed at roughly 2θ = 20.9, 25.7, 26.8, 35.4, 43.5, 57.7, 68.3, and 77.2. Furthermore, according to the literature, the clinoptilolite phase dominates in natural zeolite samples extracted from Semnan mines [47].

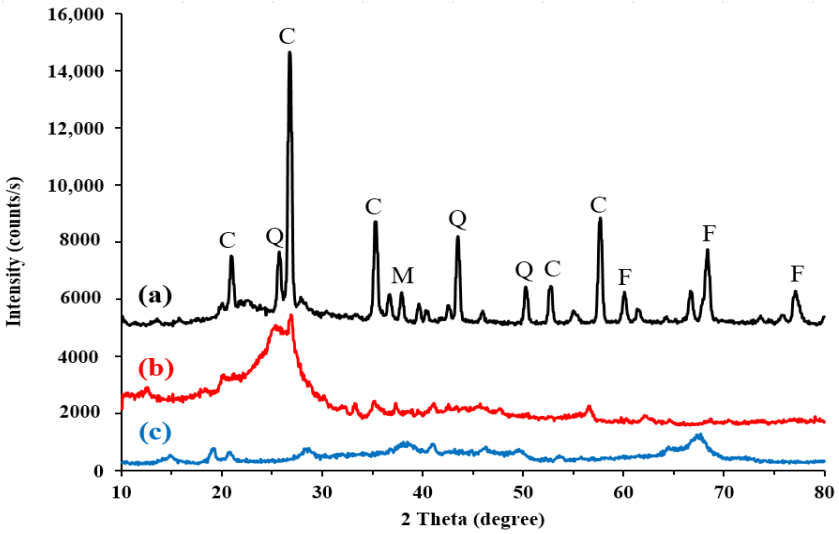

Figure 1. XRD analysis of natural zeolite (a), activated carbon (b), and activated alumina (c). Q: quartz; M: mordenite; C: clinoptilolite; F: feldspar.

Figure 1b also depicts the XRD pattern of the activated carbon. It is possible to see that the strongest peak is clearly visible in the range of 20° to 30°, while other peaks are barely noticeable. These findings are consistent with previous research [48].

The diffraction peaks of activated alumina (Figure 1c) are at 2θ = 14.9, 19.2, 20.7, 28.4, 38.1, 41.2, 46.3, 49.6, 53.6, and 67.7.

3.1.2. SEM

Samples were analyzed using scanning electron microscopy (SEM) to determine their crystal size and external morphology, as shown in Figure 2. Accordingly, average sizes of roughly 44, 34, and 38 nm were obtained respectively for zeolite, activated carbon, and activated alumina. All of the samples show agglomerated particles. However, unlike natural zeolite, showing much less granular particles, the SEM images of activated carbon and alumina demonstrate a nano-network of granular particles.

(**a**)

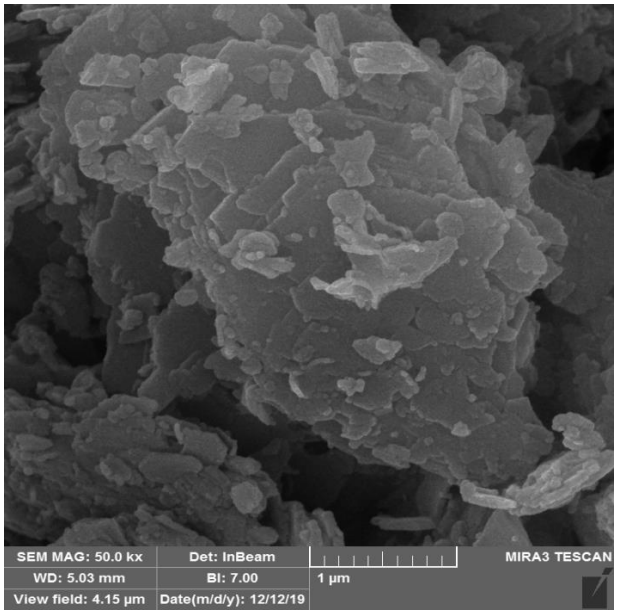

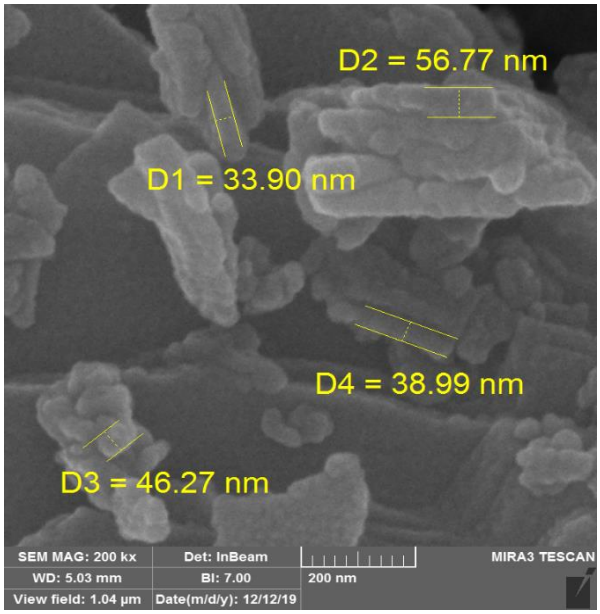

Figure 2. *Cont.*

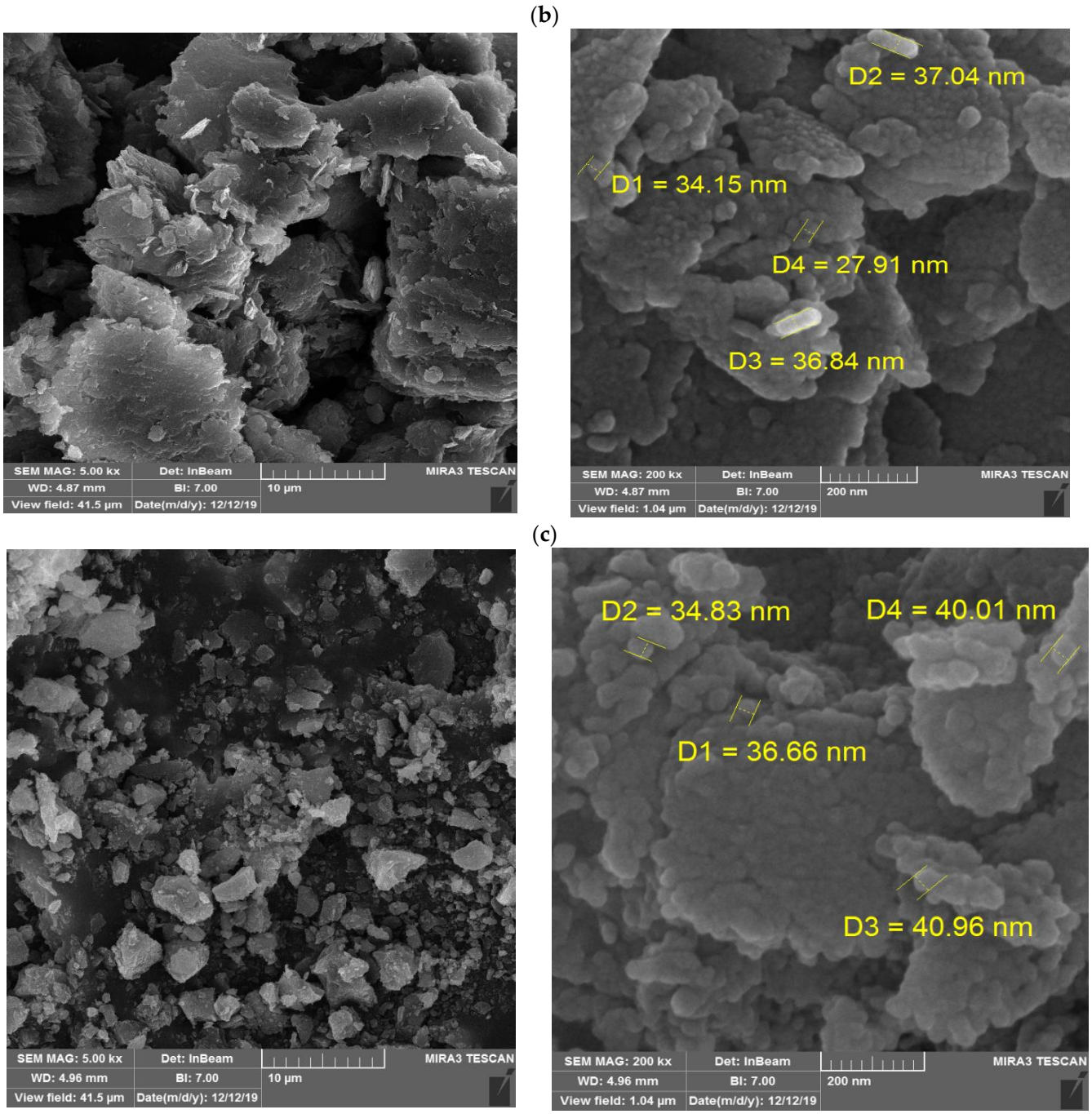

Figure 2. SEM photos for natural zeolite (**a**), activated carbon (**b**), and activated alumina (**c**).

3.1.3. BET

The BET analysis is illustrated in Figure 3 for the purpose of determining the specific surface area of natural zeolite, activated carbon, and activated alumina adsorbents. In Table 3, data on three different adsorbents' specific surface areas, average pore diameters, and specific volumes are presented. Activated carbon and activated alumina show an average pore diameter of less than 10 nm, while this parameter is more than 10 nm for natural zeolite. In addition, the specific surface area of activated carbon is 897.5 m^2/g, which is much higher than that of activated alumina (327.02 m^2/g) and natural zeolite (19.87 m^2/g). This is most likely because the natural zeolite and activated alumina used are raw minerals extracted from mines, whereas activated carbon is prepared through a process that automatically increases its specific surface area. Activated carbon has a specific

pore volume that is 1.3 times greater than that of natural zeolite and 3.7 times smaller than that of activated alumina, but its average pore diameter is only 2.0 nm, making it smaller than both alumina (5.3 nm) and natural zeolite (11.7 nm) in structure.

(**a1**)

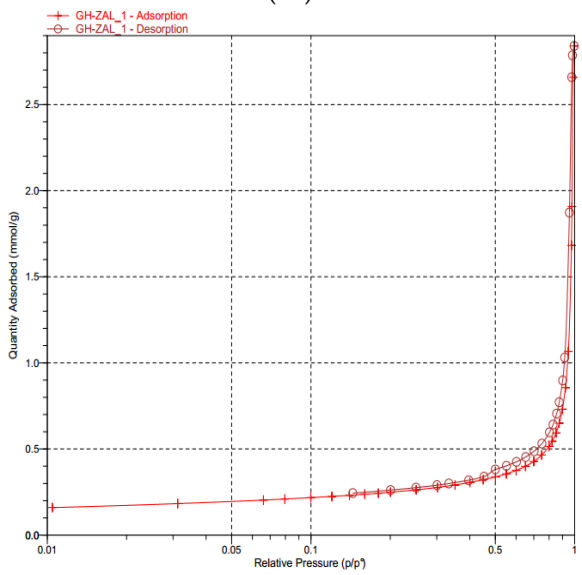

(**a2**)

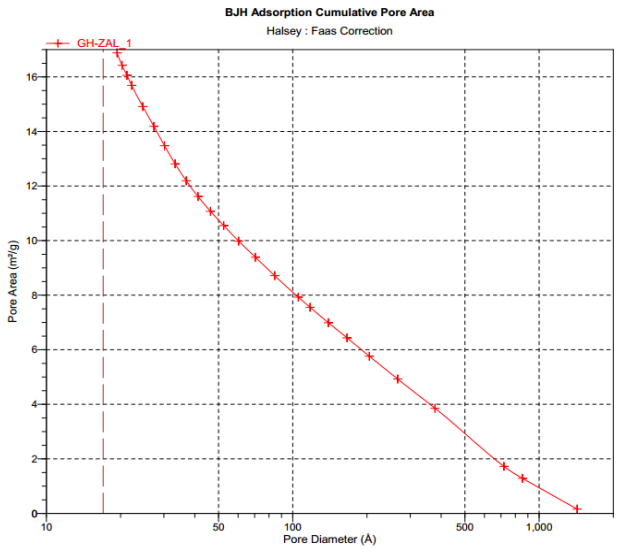

(**b1**)

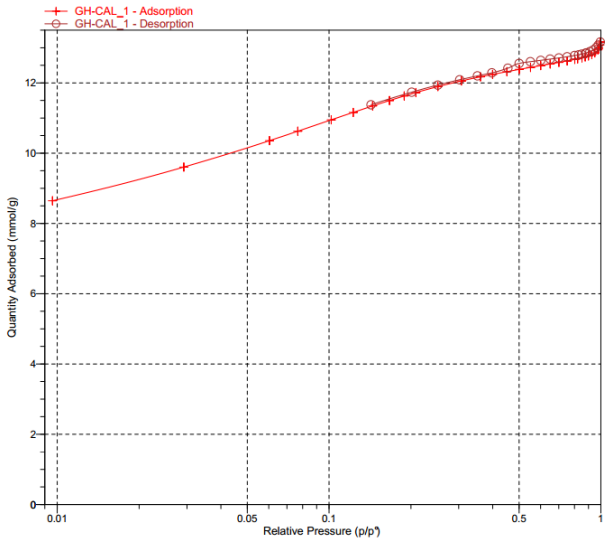

(**b2**)

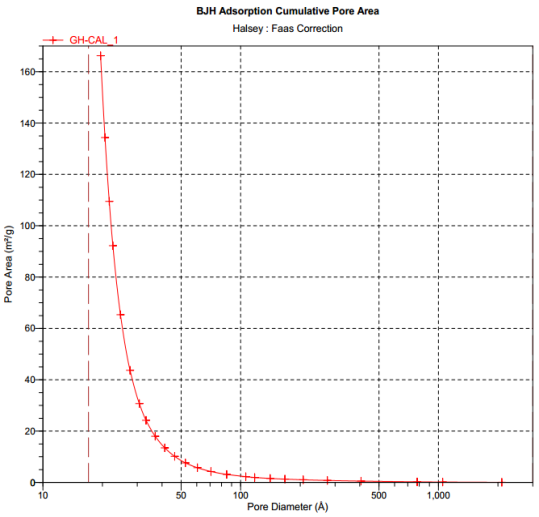

Figure 3. *Cont.*

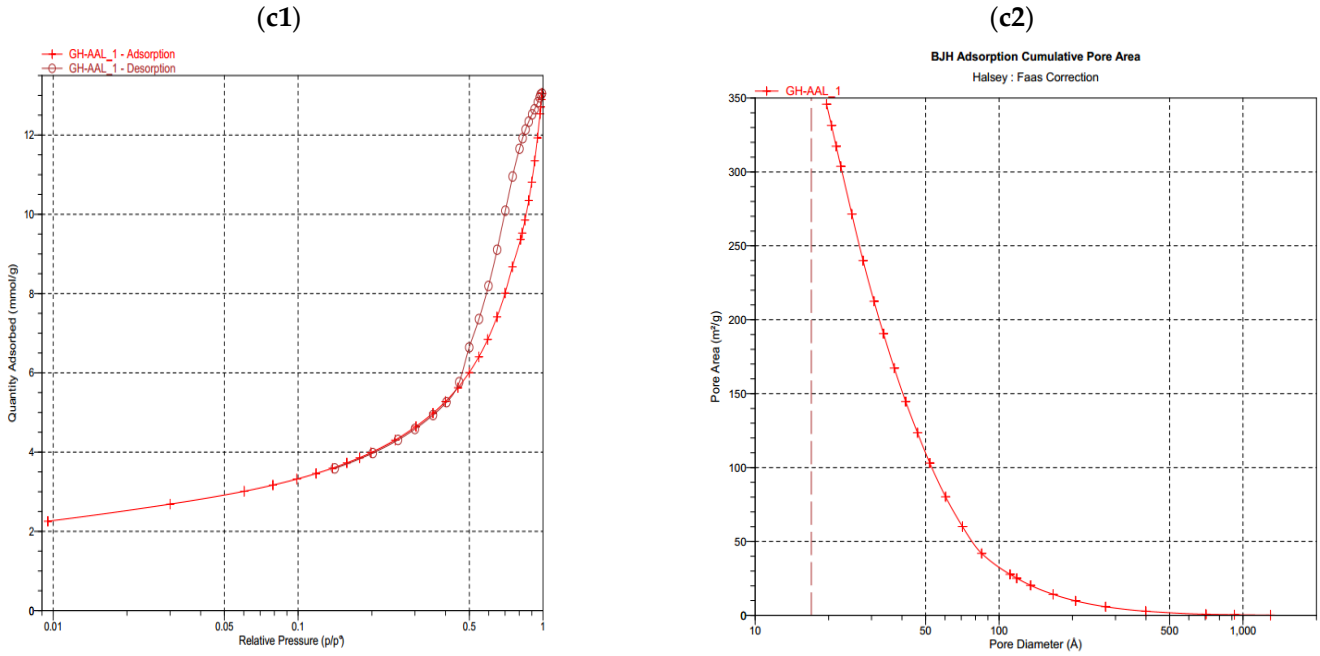

Figure 3. BET analysis: (**1**) adsorption/desorption curve and (**2**) cumulative pore area curves for natural zeolite (**a**), activated carbon (**b**), and activated alumina (**c**).

Table 3. Specific surface area, average pore diameter, and specific pore volume of adsorbents.

Parameter	Natural Zeolite	Activated Carbon	Activated Alumina
Specific pore volume (cm^3/g)	0.098	0.128	0.48
Average pore diameter (nm)	11.7	2	5.3
Specific surface area (m^2/g)	19.87	897.5	327.02

3.2. Reducing Water Hardness with Low-Cost Adsorbents and Their Modified Forms

To remove hardness ions (calcium and magnesium) from drinking water and groundwater, zeolite, activated carbon, and activated alumina were used as adsorbents. Then, these adsorbents were modified separately with salt and acid sequentially (salt–acid), and finally, the performance of each adsorbent was evaluated separately.

3.2.1. Natural Zeolite Clinoptilolite Type

The parameters of total hardness removal (%), removal of calcium and magnesium ions (%) as a function of different contact times (10, 20, 30, 60, 90, and 120 min), various concentrations of natural zeolite (20, 40, 60, and 80 g/L), and modified zeolite with the corresponding concentration (determined from the plot) for each water sample under constant experimental conditions (constant initial ion concentration, a rotation speed of 150 rpm, and a temperature of 30°C) are illustrated (Figures 4–6). The complexometry method with EDTA was also used to determine the total hardness and Ca and Mg hardness in water. The results of the experiments carried out are as follows.

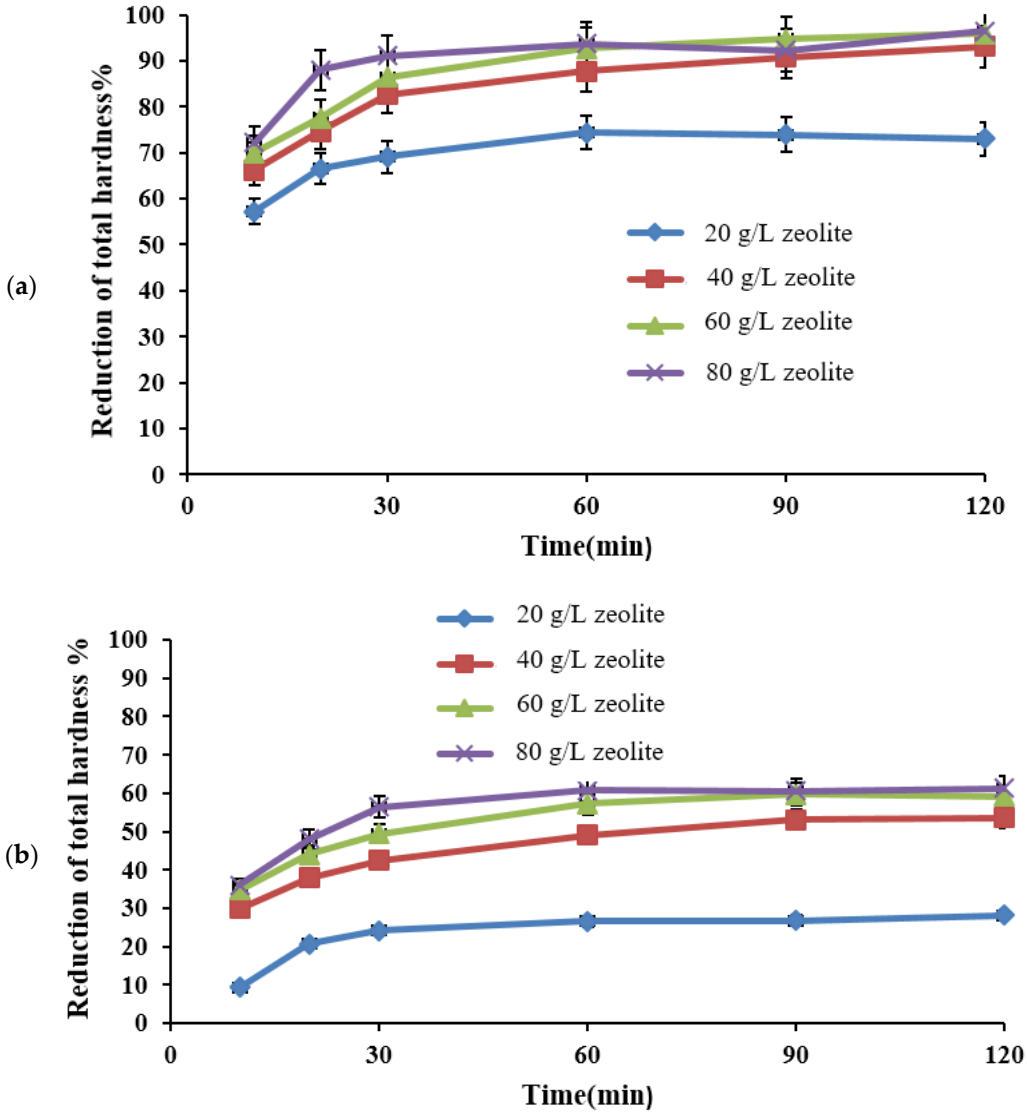

Figure 4. The effect of contact time on the reduction in total hardness (%) of (**a**) drinking water and (**b**) groundwater by natural zeolite.

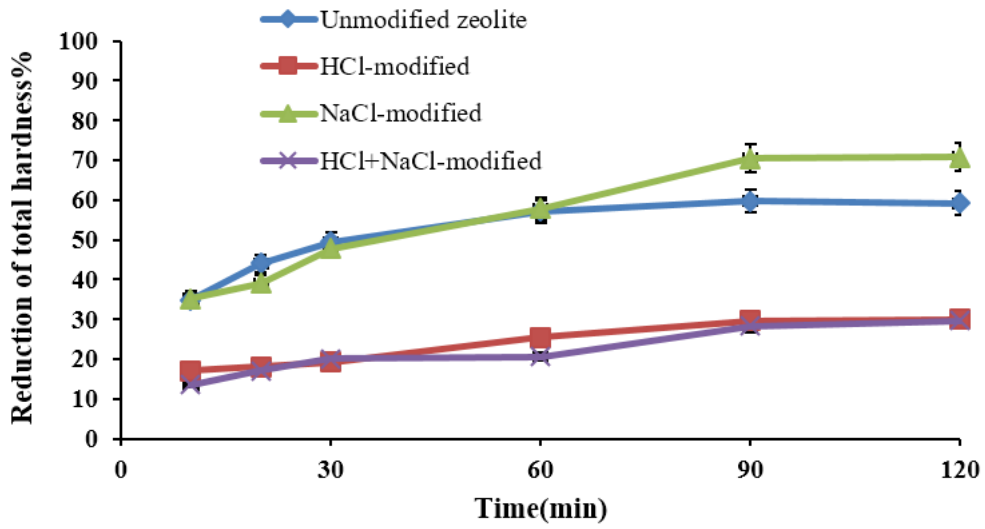

Figure 5. The effect of contact time on the decrease in total hardness (%) for groundwater by modified zeolite at 60 g/L.

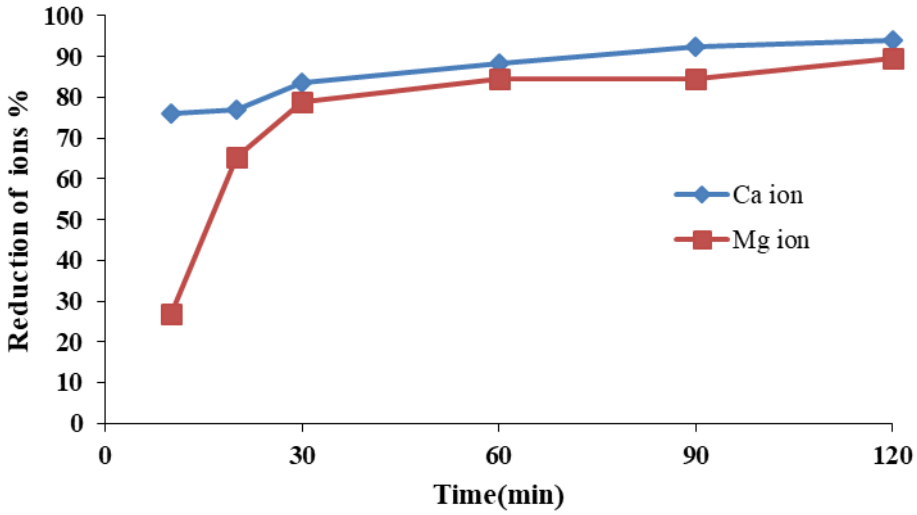

Figure 6. The effect of contact time in decreasing calcium and magnesium ions (%) in drinking water with natural zeolite at a concentration of 40 g/L.

The Effect of Zeolite in Reducing Total Hardness

Figure 4a,b exhibit the effect of contact time on the percent removal of total hardness at different concentrations of natural zeolite. Figure 4a shows that as the contact time was prolonged, the percent removal of total hardness also increased. This process continued until equilibrium was reached and remained unchanged. This phenomenon can be explained by the fact that at the beginning of the ion exchange process, as the contact time increases, the adsorbed particles have more opportunities to penetrate the adsorbent and occupy the active adsorption sites. However, when the process reaches equilibrium, the adsorbent is saturated and filled. Therefore, when the empty sites are filled, prolonging the contact time does not affect the adsorption efficiency. Accordingly, increasing the contact time by more than 90 min did not affect the removal efficiency. Therefore, the best contact time in this experiment can be considered 90 min. Plots show that total hardness removal (%) was 73.07%, 93.07%, 95.84%, and 96.42% at concentrations of 20, 40, 60, and 80 g/L zeolites, respectively. Therefore, according to the results, a concentration of 40 g/L for the ion exchange process can be considered suitable for drinking water. The same concentration order for the removal of total hardness of groundwater was found to be 28.22%, 53.65%, 59.23%, and 61.32%, respectively. Therefore, the appropriate concentration during the ion exchange process for groundwater can be considered 60 g/L. Thus, it can be assumed that this zeolite can effectively remove hardness from drinking water and groundwater.

The Effect of Natural and Modified Zeolite in Reducing the Total Hardness in Groundwater

The effect of contact time on the removal of total hardness by natural and modified zeolite at a concentration of 60 g/L for groundwater is depicted in Figure 5. For salt-modified zeolite, the total hardness removal in 90 min was 70.38%, while for natural zeolite in 90 min, it was 59.74%. Sodium ions are exchanged for exchangeable ions of zeolite by cation exchange, and adsorbent sites become uniform with sodium, which boosts the adsorption capacity. However, it was observed that modification of zeolite with acid reduced the adsorption capacity. When zeolites were activated with acid, it was expected that the acid would remove metal oxides and unwanted substances from the zeolite in addition to ion exchange, creating a porous structure and a high specific surface area that would boost the adsorption capacity. However, this did not happen in our experiment. The possible reason could be that the acid destroys certain adsorbent sites due to the partial dissolution of Si tetrahedrals and the free bonds formed that created new micropores.

On the one hand, if the aim is to adsorb polar molecules, which was polar calcium carbonate in this experiment, it will reduce the ion exchange capacity. On the other hand,

modifying the zeolite with acid can be effective if the purpose is to adsorb nonpolar molecules. Due to the high removal of the total hardness of the drinking water by zeolite, the modification of zeolite for drinking water was omitted.

The Effect of Natural Zeolite in Decreasing Calcium and Magnesium Ions in Drinking Water

Figure 6 shows that the removal of Ca and Mg during the early period increases until equilibrium is reached. Due to the large number of active zeolite sites reacting with the ions, the initial adsorption rate is very fast. As a result, the adsorption rate on the zeolite surface increases rapidly.

The reactions carried out during the ion exchange process to remove carbonate hardness are as follows. Z stands for zeolite.

$$Ca(HCO_3)_2 + Na_2Z \rightarrow CaZ + 2NaHCO_3 \quad (16)$$

$$Mg(HCO_3)_2 + Na_2Z \rightarrow MgZ + 2NaHCO_3 \quad (17)$$

3.2.2. Activated Carbon

The reduction in the total hardness parameter as a function of the different contact times (10, 20, 30, 60, 90, and 120 min) is depicted (Figure 7a,b). The conditions for performing these tests were the same as those required for the zeolite tests described in Section 3.2.1. In this stage, the adsorbent used was activated carbon and its modified form.

The Effect of Activated Carbon on Reducing Total Hardness

Figure 7a,b present the effect of contact time on the total hardness removed for both water samples at different concentrations of activated carbon. The best contact time (90 min) and the time to reach equilibrium to achieve this phenomenon are similar to the zeolite adsorbent. The plot shows that the percent removal of total hardness with 20, 40, 60, and 80 g/L activated carbon was 11.57%, 17.94%, 30.76%, and 33.91%, respectively. Therefore, according to the results, it can be concluded that the best concentration in this experiment for drinking water was 60 g/L. This activated carbon is relatively well suited for removing water hardness due to its good removal efficiency.

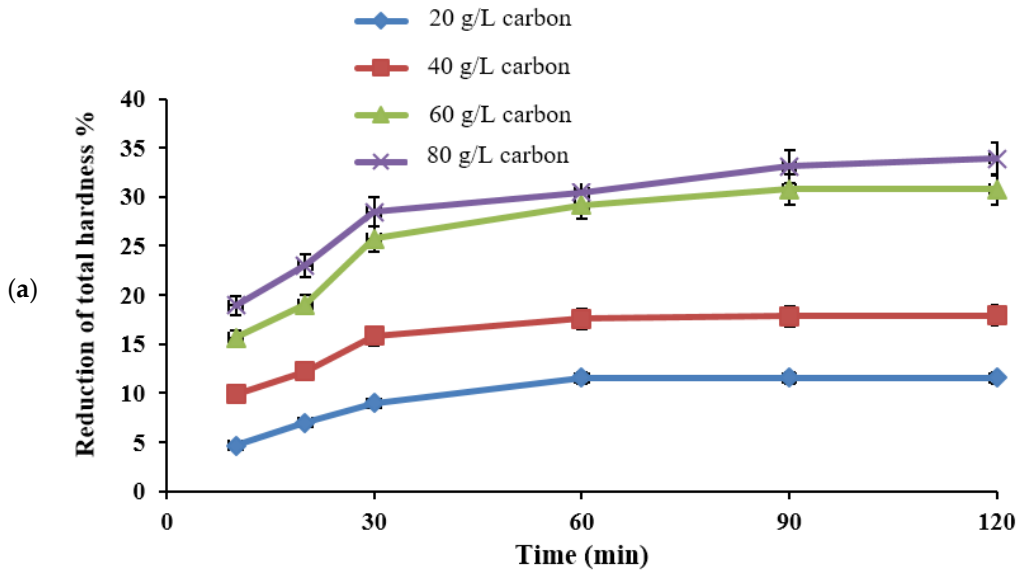

Figure 7. *Cont.*

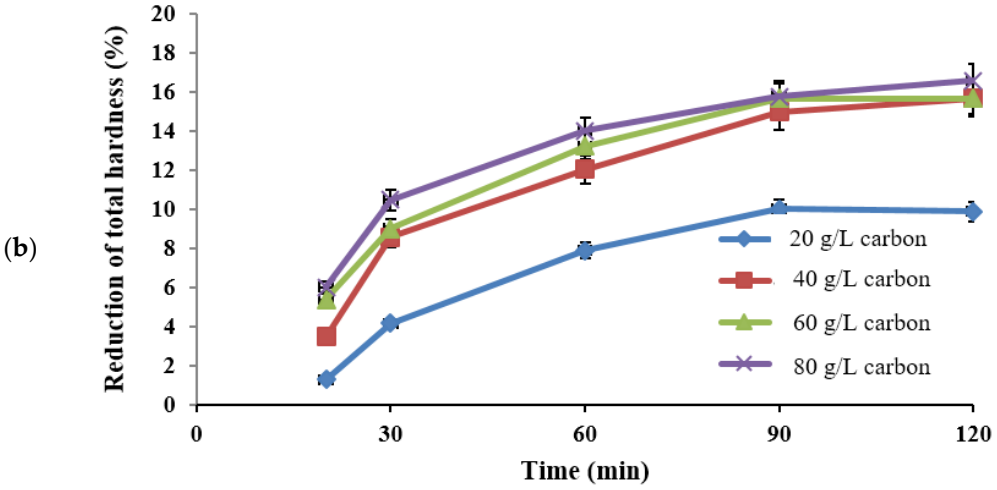

Figure 7. The effect of contact time on reducing total hardness (%) of (**a**) drinking water and (**b**) groundwater by different concentrations of activated carbon (g/L).

Figure 7b illustrates the effect of contact time on reducing total hardness (%) for the groundwater. It was found that the removal of total hardness with 20, 40, 60, and 80 g/L activated carbon was 9.89%, 15.67%, 15.67%, and 16.58%, respectively. Thus, it can be argued that the optimum concentration in this experiment for groundwater was 40 g/L.

The Effect of Modified Activated Carbon on the Reduction in Total Hardness

The effect of contact time on removing total hardness by modified activated carbon is shown in Figure 8a,b. Hardness reduction was enhanced in each water sample as the contact time increased. In addition, the removal of adsorbed metal ions increased rapidly for different forms of modified adsorbents during the early period until equilibrium was reached. Any modification of activated carbon was effective in reducing the total hardness of drinking water (Figure 8a). The modification of carbon with acid and salt reduced the total hardness of drinking water by 40.19% and 33.07%, respectively. The highest removal of total hardness was associated with successive modifications with salt and acid. This modification reduced the total hardness by 41.53%, which is 10.77% more than the unmodified adsorbent. According to Figure 8b, the activated carbon modified with acid and the activated carbon modified with salt and acid did not significantly differ from the unmodified form, while the activated carbon modified with salt reduced the total hardness by 25.43%, which is 9.76% more than the unmodified activated carbon form for the groundwater sample. It can be argued that activated carbon modification with salt effectively removes high hardness, and modification with salt and acid is potent in reducing hardness in drinking water. Equilibrium was reached in 90 min for each plot. After that, increasing the contact time did not affect hardness removal.

The Effect of Natural and Modified Activated Carbon on Decrease in Calcium and Magnesium Ions

As shown in Figures 9 and 10, activated carbon and its modified form removed calcium and magnesium ions from drinking water at a concentration of 60 g/L. Sequential acid–salt modification and acid modification of activated carbon were more suitable for the adsorption of calcium ions. The results showed that acid-modified activated carbon removed 47.11% of calcium ions, which is 11.54% more than the unmodified form. In drinking water, activated carbon and acid-activated carbon reduced the concentration of magnesium (Figure 10). In contrast, salt-modified activated carbon and successive salt–acid-modified carbon decreased the magnesium concentration by 18.26% and 26.91%, respectively.

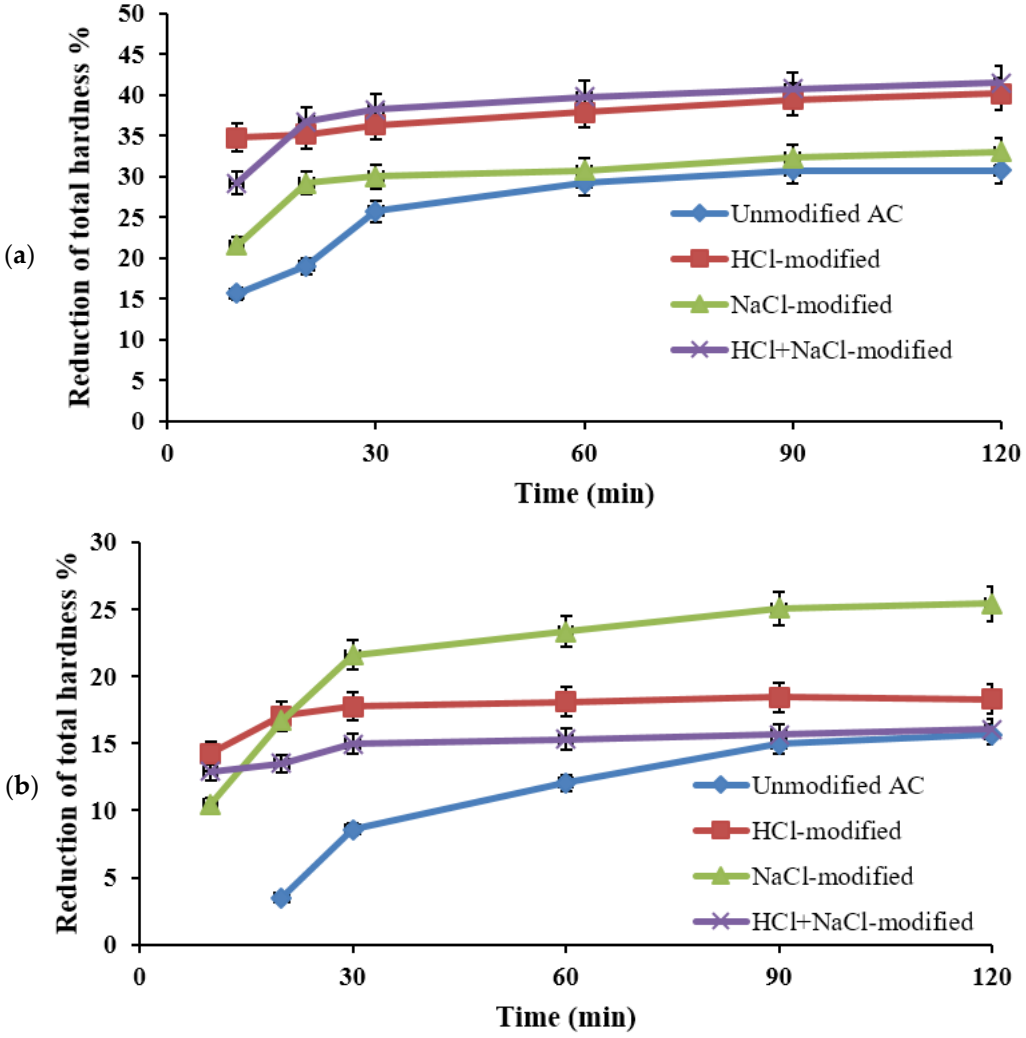

Figure 8. The effect of contact time on the decrease in total hardness (%) of (**a**) drinking water by modified activated carbon (AC) with a concentration of 60 g/L and (**b**) groundwater by modified activated carbon with a concentration of 40 g/L.

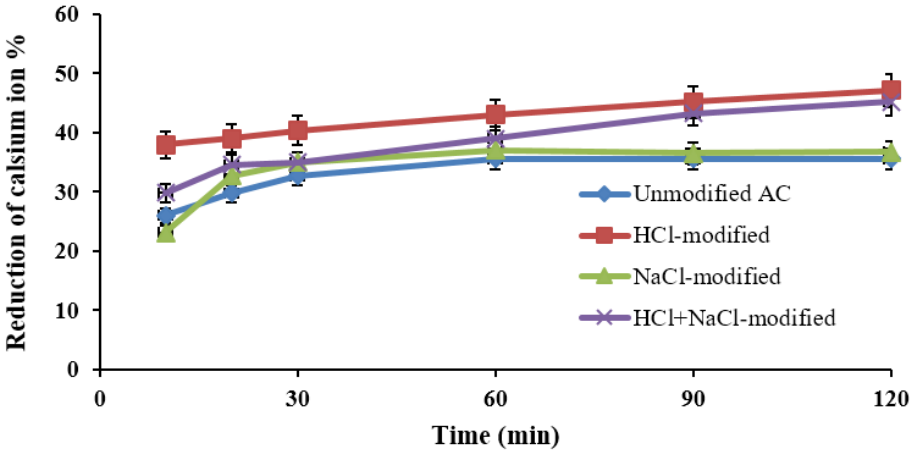

Figure 9. The reduction in calcium ions in drinking water versus time using activated carbon and modified forms.

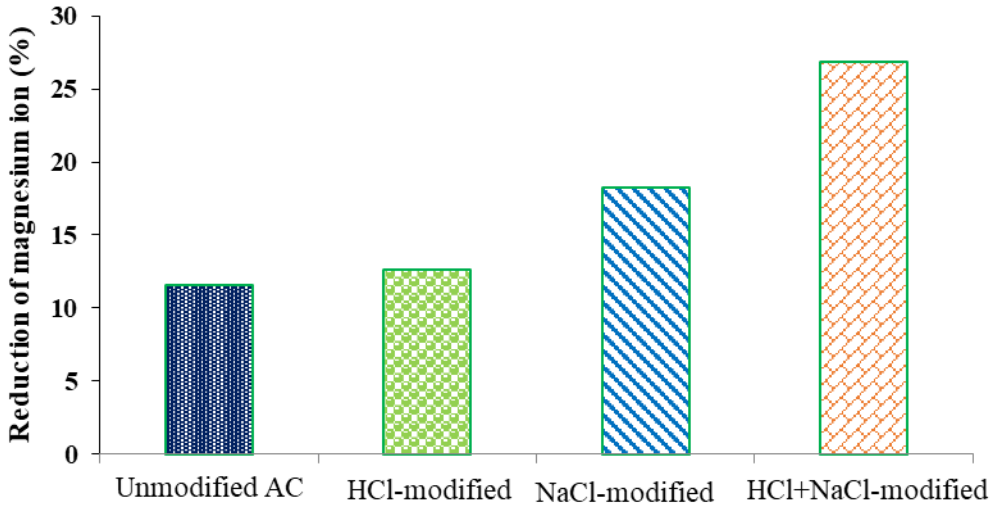

Figure 10. The decrease in magnesium in drinking water by activated carbon and its modified form.

3.2.3. Activated Alumina

Figures 11 and 12 illustrate the reduction in total hardness parameters and Ca and Mg ions as a function of the different contact times (10, 20, 30, 60, 90, and 120 min). The conditions for performing these experiments were the same as those described in the previous sections for activated carbon and zeolite. Activated alumina and its modified form were used, and their results are reported in this section.

The Effect of Activated Alumina on Reducing Total Hardness

Figure 11a,b depict the total hardness removed from drinking water and groundwater samples at different concentrations of activated alumina based on contact time. The optimal contact time (90 min) and the time to reach equilibrium to realize this phenomenon are similar to those of the zeolite adsorbent. Figure 11a reveals that total hardness removal at different concentrations of 20, 40, 60, and 80 g/L alumina was 40.76%, 47.69%, 56.92%, and 58.46%, respectively. Therefore, according to the results, it can be concluded that the suitable concentration in this experiment was 60 g/L. Figure 11b shows that the decrease in total hardness rose with increasing contact time, which continued until equilibrium was reached and then did not change significantly. Thus, by enhancing the contact time beyond 90 min, the removal efficiency is not affected, and the optimal contact time is considered to be 90 min. The removal of total hardness with 20 g/L alumina was 26.13%, with 40 g/L alumina was 39.72%, with 60 g/L alumina was 41.46%, and with 80 g/L alumina was 44.64% (Figure 11b). Thus, according to the results, the concentration of 40 g/L was the appropriate one in this experiment.

The Effect of Modified Activated Alumina on the Decrease in Total Hardness

Figure 12a,b show the effect of contact time on total hardness removal by modified activated alumina for both drinking water and groundwater samples. Compared to the unmodified form, salt-modified activated alumina did not affect total hardness removal. Even modification of alumina with acid and salt–acid reduced the ability of alumina to adsorb hardness ions. This may be due to the alumina dissolving in the acid because, after each modified alumina test with the acid, the water sample's color turned white. However, other modifiers must be sought to increase the adsorption capacity of alumina.

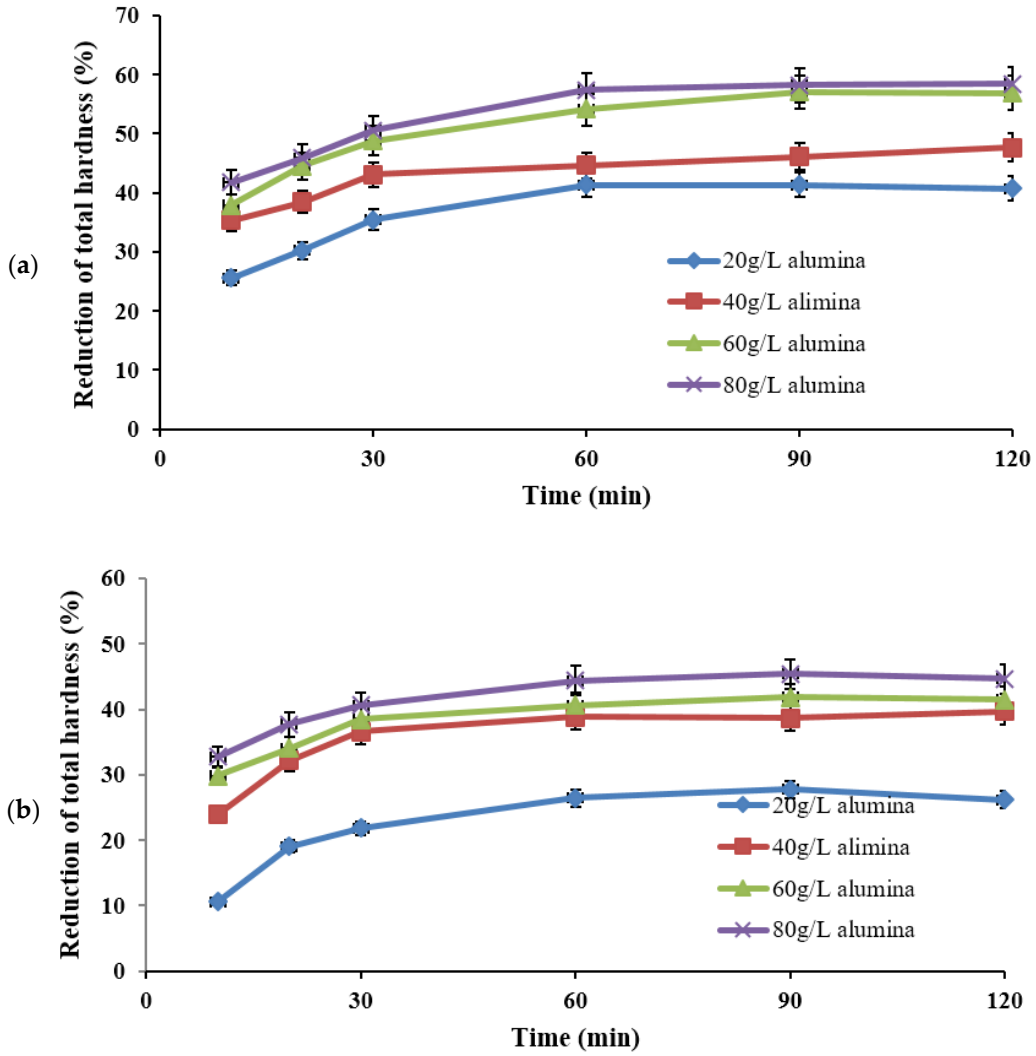

Figure 11. The effect of different concentrations of activated alumina (g/L) on reducing total hardness (%) of (**a**) drinking water and (**b**) groundwater.

The Effect of Activated Alumina in Reducing Calcium and Magnesium Ions in Drinking Water

According to Figure 13, the removal of calcium and magnesium ions increased over time. At a concentration of 60 g/L alumina, 46.15% of calcium and 30.31% of magnesium ions were removed in 90 min. Because of the impact of ion hydration energy, calcium was adsorbed at a higher rate than magnesium. Due to the higher charge per unit volume of magnesium ions compared to calcium ions, magnesium ions' hydration energy is higher. Moreover, since a hydrated ion must lose its water molecules during the exchange, the exchange rate of the magnesium ion is lower.

3.3. The Most Suitable Adsorbent

The efficiency of three adsorbents, namely, zeolite, activated carbon, and activated alumina, and their efficient modified forms was evaluated under the same experimental conditions for reducing the total hardness of drinking water and groundwater. The results under optimum conditions (optimum concentration and contact time of 90 min, rotation speed of 150 rpm, and temperature of 30 °C) are shown in Figure 14a,b. For different adsorbents, their efficiency is as follows:

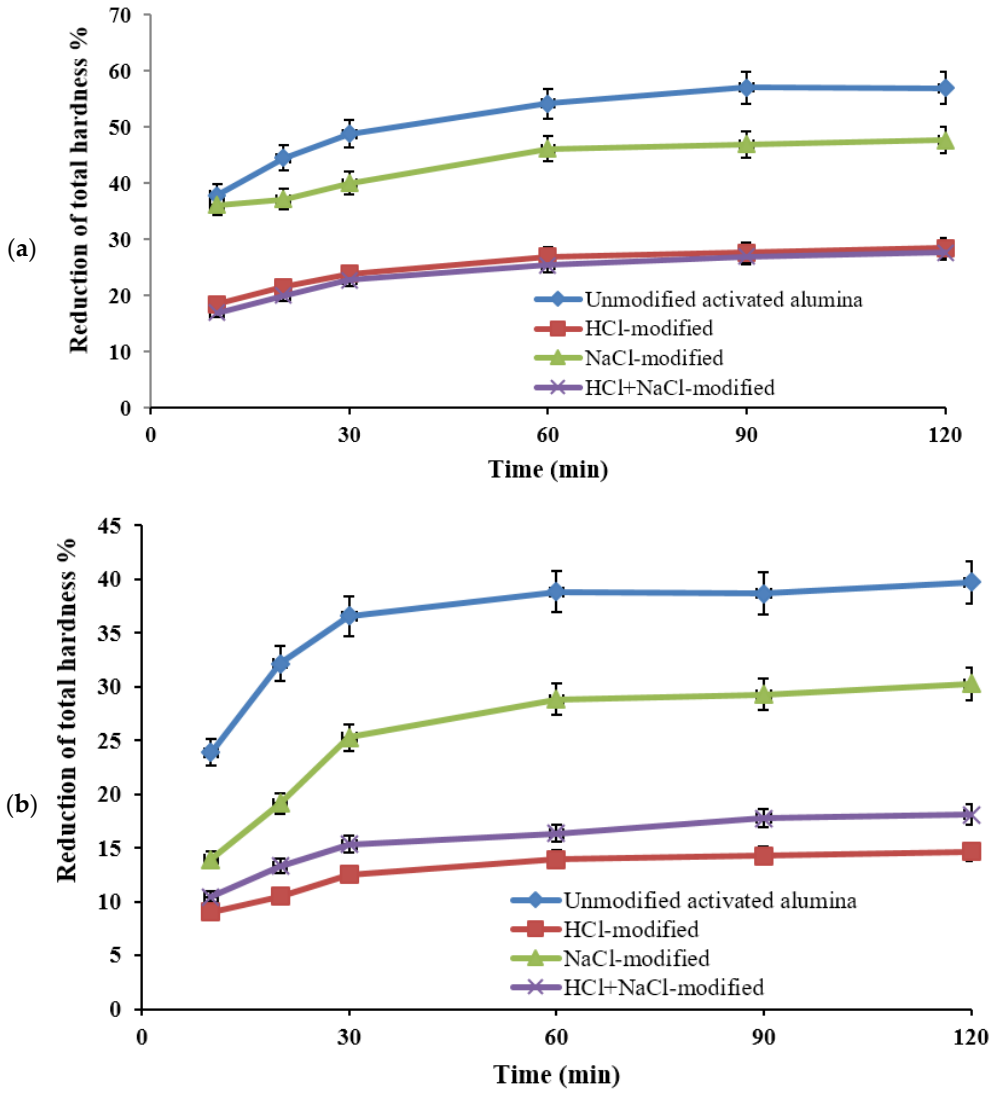

Figure 12. The effect of contact time on the decrease in total hardness (%) of (**a**) drinking water by modified activated alumina with a concentration of 60 g/L and (**b**) groundwater by modified activated alumina with a concentration of 40 g/L.

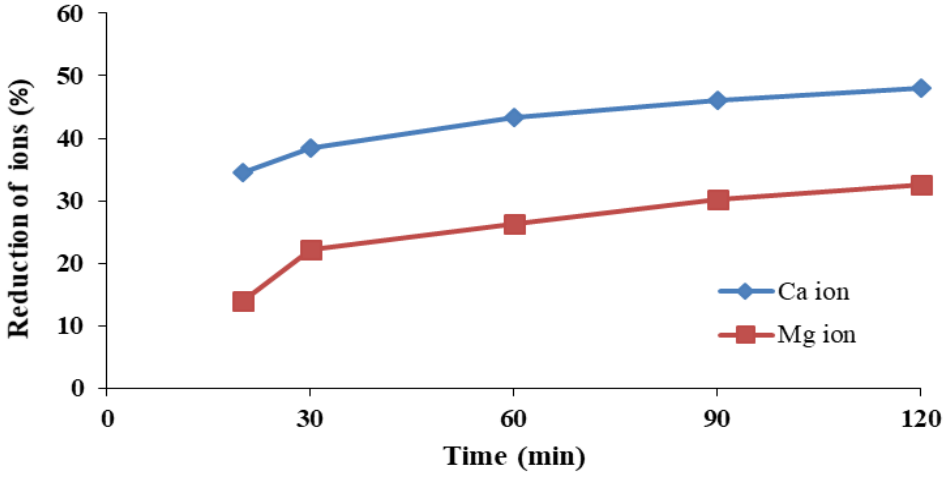

Figure 13. The effect of activated alumina in reducing calcium and magnesium ions in drinking water.

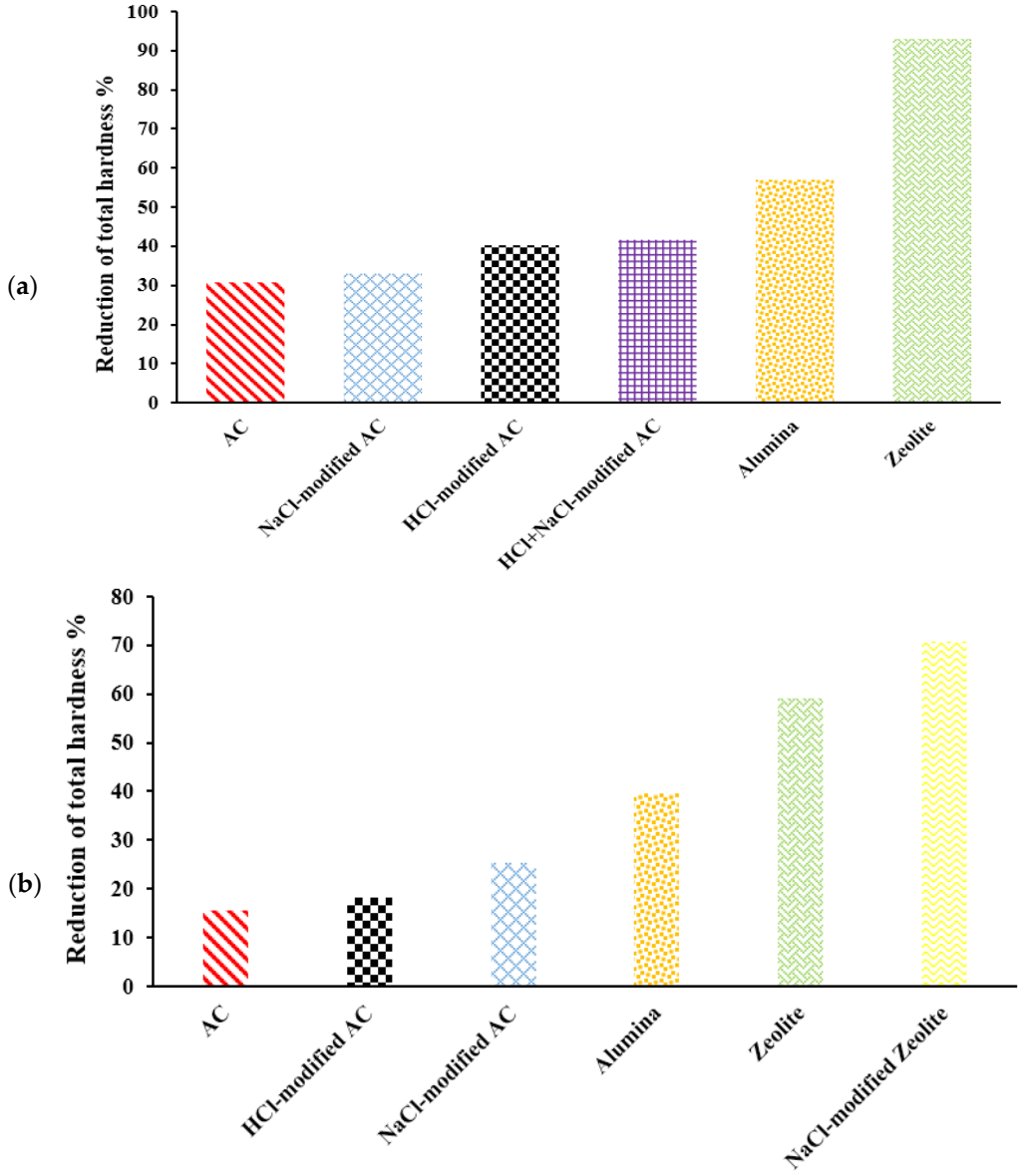

Figure 14. Comparison of reduction in the total hardness of (**a**) drinking water and (**b**) groundwater with natural and modified adsorbents under optimal conditions.

Drinking water: zeolite > non-modified alumina > HCl-NaCl-modified activated carbon > HCl-modified activated carbon > NaCl-modified activated carbon > non-modified activated carbon.

Groundwater: NaCl-modified zeolite > non-modified zeolite > non-modified alumina > NaCl-modified activated carbon > HCl-modified activated carbon > non-modified activated carbon.

According to the findings, among the various adsorbents, zeolite and salt-modified zeolite are the best, with the highest percentages in reducing the total hardness of drinking water and groundwater, respectively. On the other hand, the lowest reduction in total hardness for both samples was recorded for activated carbon.

3.4. Adsorption Equilibrium Results

3.4.1. Langmuir Isotherm Model

By plotting the linear graph C_e/q_e as a function of C_e, the constant values q_{max} and K_L, which represent the slope and intercept, can be obtained from the experimental data using the linear equation. These plots are shown in Figure 15a–c. The obtained constants q_{max}

and K_L with the correlation coefficient R^2, which shows the conformity of the experimental data with the Langmuir isotherm model, are listed in Table 4. Since the concentration of magnesium ions was lower than that of calcium ions, and both hardness ions behaved in almost the same way, most of the research focused on calcium ions. The equilibrium data obtained for all three adsorbents used in these experiments (zeolite, activated carbon, and activated alumina) under experimental conditions (constant initial concentration, optimum contact time of 90 min, different concentrations (20, 40, 60, and 80 g/L) of the adsorbents mentioned above, a rotation speed of 150 rpm, and a temperature of 30 °C) were fitted to the linear Langmuir plot (Figure 15a–c). It can also be seen that among the three adsorbents used in the experiments, zeolite was well fitted to the linear Langmuir plot with a higher correlation coefficient (R^2 = 0.9925) compared to the other adsorbents. This suggests that the Langmuir isotherm may be a suitable model to describe the adsorption reaction mechanism of calcium ions by zeolite. This suggests that the Langmuir hypothesis of the homogeneous distribution of active sites on the zeolite surface is valid. Ion exchange can also be included in the Langmuir model. The Langmuir model differs from the ion exchange method in that the latter assumes that all ion-binding sites are initially occupied. It is also possible to describe the nature of the adsorption process with a separation factor R_L, as shown in Equation 11. In the case of the adsorption of calcium ions by zeolite, R_L was 0.0632, which is between 0 and 1. Thus, this value indicates the feasibility and desirability of the adsorption process of calcium ions from an aqueous solution with zeolite.

Table 4. Correlation coefficient and constant values of the isotherms for the adsorption of calcium ions by different adsorbents.

Adsorbents	Langmuir			Freundlich			Temkin		
	R^2	q_{max} (mg.g^{-1})	c	R^2	n	K_F (mg.g^{-1})	R^2	B	K_T
Zeolite clinoptilolite	0.9925	7.485	0.088	0.9887	4.521	1.733	0.9073	1.844	0.596
Activated alumina	0.9599	1.285	0.112	0.5681	1.253	0.048	0.849	0.728	0.057
Activated carbon	0.8688	0.901	0.227	0.8558	3.599	0.225	0.9014	0.237	0.437

3.4.2. Freundlich Isotherm Model

Using the linear equation obtained from the experimental data, the values of n and K_F, representing the slope and intercept, can be determined by drawing a linear plot of log (q_e) versus log (C_e) (Figure 16a–c). Table 4 also shows the calculated values of the constants n and K_F and the correlation coefficient R^2, representing the experimental data fitted to the Freundlich isothermal model. The experimental equilibrium data for all three adsorbents used in these experiments were obtained under the same conditions as mentioned in Section 3.4.1. The observed correlations are fitted to the linear Freundlich plot. It also shows that the linear form of the Freundlich isotherm fits well only for one of the three adsorbents used in the adsorption experiments, namely, zeolite, with a correlation coefficient of R^2 = 0.9887 compared to the other two. Therefore, the Freundlich isotherm can be used as a suitable model to describe the adsorption of calcium ions by zeolite. According to the calculated constant value n given in Table 4, which ranges from 2 to 10, the adsorption of calcium ions by natural zeolite is a desirable process with suitable adsorption properties.

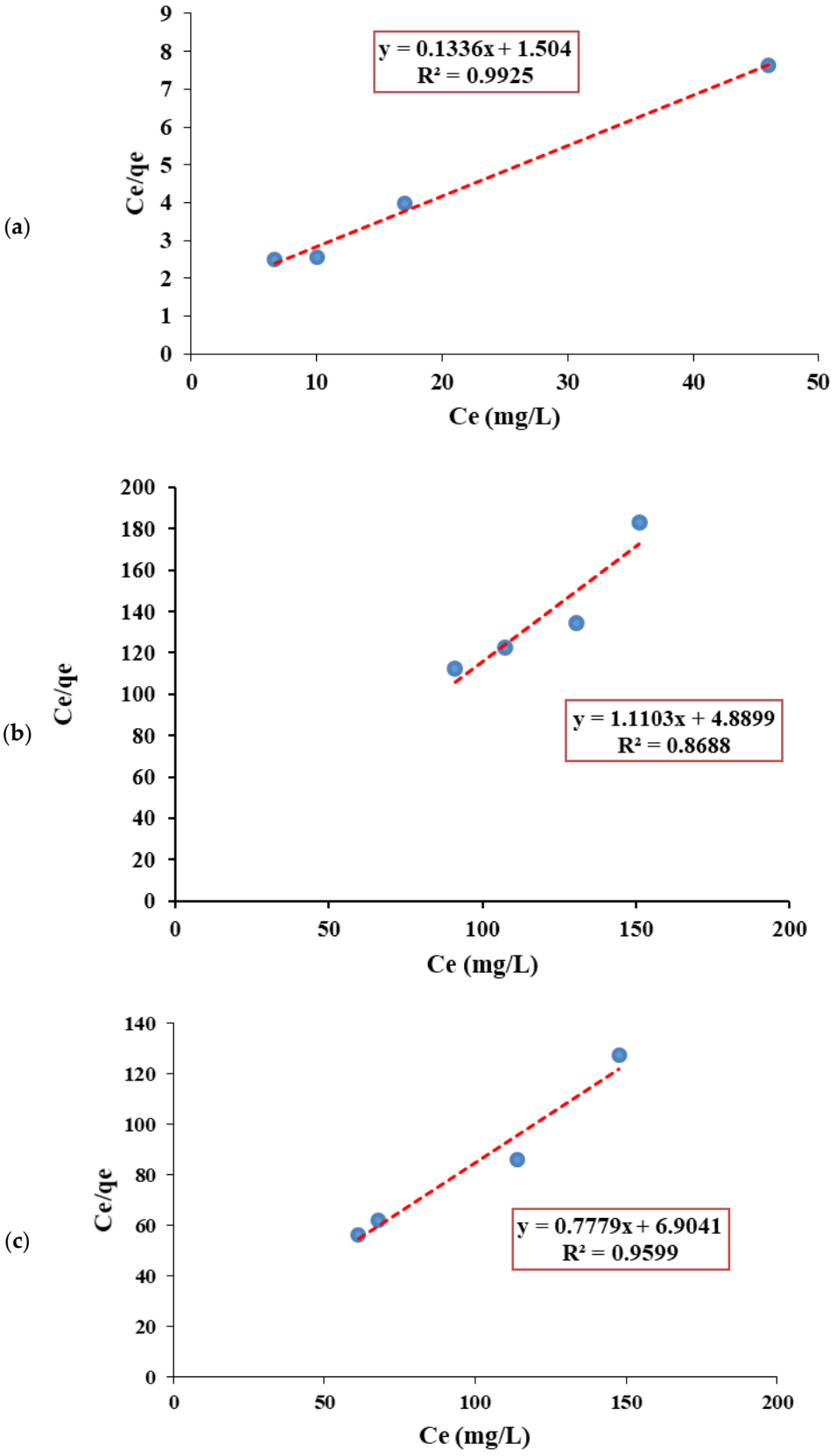

Figure 15. Linear form of Langmuir isotherm model for the adsorption of calcium ions by (**a**) zeolite, (**b**) activated carbon, and (**c**) activated alumina.

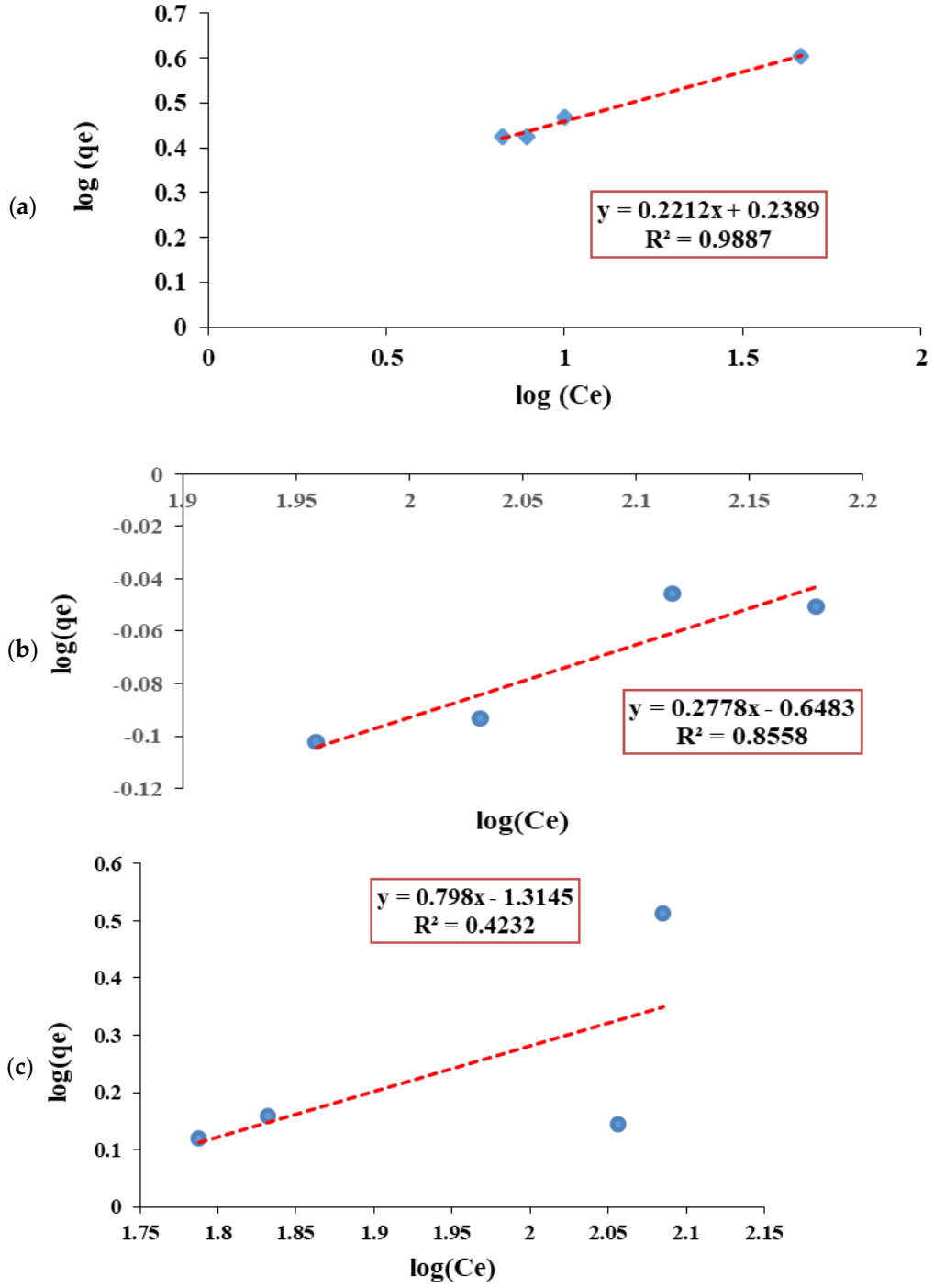

Figure 16. Linear form of Freundlich isotherm model for the adsorption of calcium ions by (**a**) zeolite, (**b**) activated carbon, and (**c**) activated alumina.

3.4.3. Temkin Isotherm Model

By drawing a linear graph of q_e versus ln (C_e), the values of B and K_T, which represent the slope and intercept, respectively, can be obtained from the linear equation of the experimental data (Figure 17a–c). Table 4 also shows the calculated values of the constants B and K_T and the correlation coefficient R^2. The experimental data for all three adsorbents used in these adsorption experiments were fitted to the linear plot of Temkin based on the observed correlation coefficient. Among the three adsorbents used in the adsorption experiments, the zeolites had a higher correlation coefficient, R^2 = 0.9073, than the other adsorbents. Thus, the Temkin isotherm is a relatively suitable model to describe the

adsorption process of calcium ions by zeolite. A comparison of the correlation coefficients of Langmuir, Freundlich, and Temkin models shows that the Langmuir isotherm model more accurately describes the equilibrium of the adsorption process of calcium ions by zeolite.

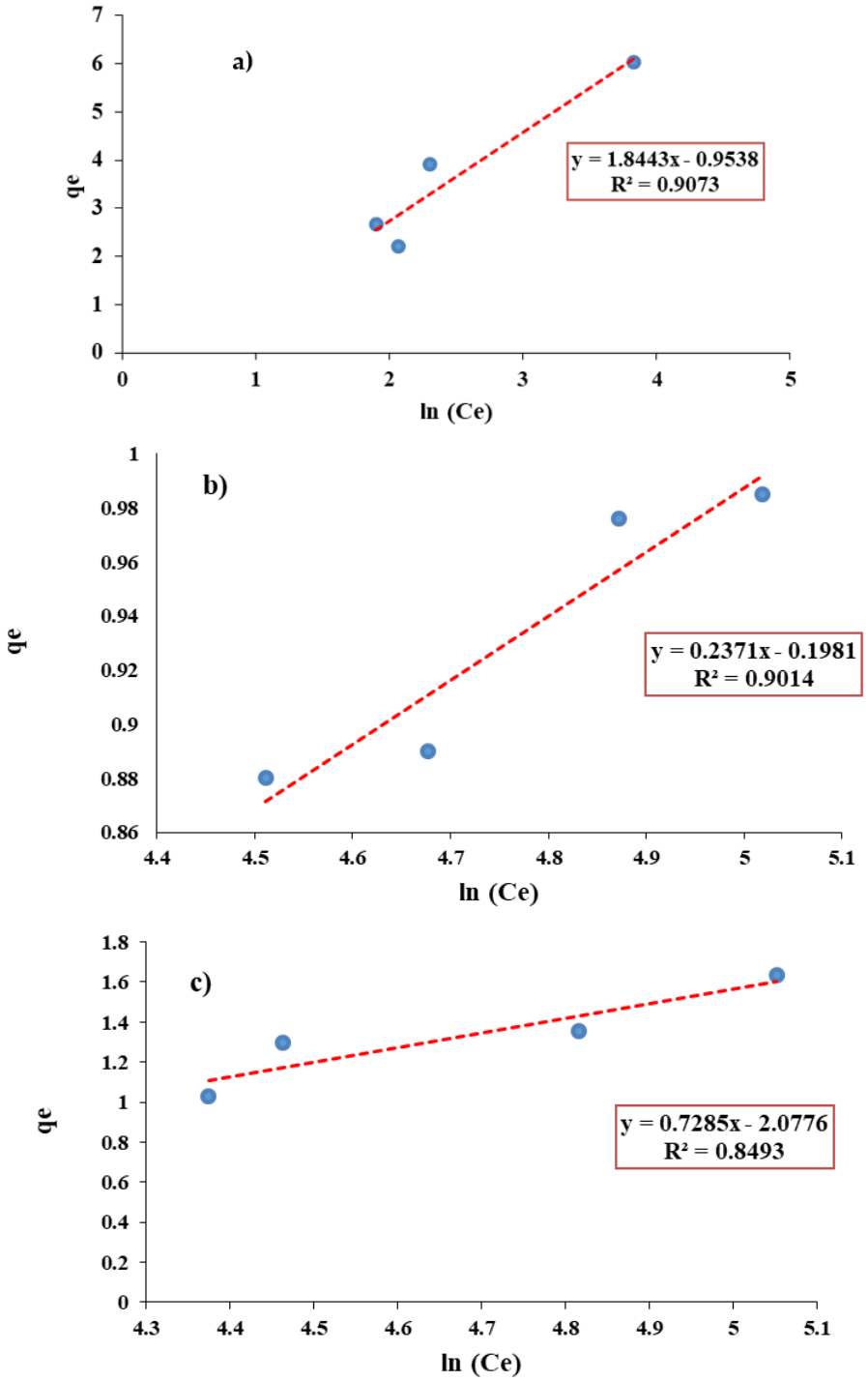

Figure 17. Linear form of Temkin isotherm model for the adsorption of calcium ions by (**a**) zeolite, (**b**) activated carbon, and (**c**) activated alumina.

The results of the study of the adsorption isotherms, including the desired constants and their correlation coefficients, are documented in Table 4. When the equilibrium process of calcium ion adsorption using different adsorbents was studied, it was found that the experimental data of zeolite fit linear graphs with a relatively high correlation coefficient

compared to the other adsorbents used. Therefore, comparing the studied models for zeolite, it is clear that the Langmuir model describes the adsorption process better than the two other models. Therefore, Langmuir isotherms with high correlation coefficients (R^2 = 0.9925) are more suitable for predicting adsorption behavior than the Freundlich and Temkin models.

3.5. Adsorption Kinetic Results

3.5.1. Pseudo-First-Order Kinetic Model

Figure 18a–c depict the linear plot of log (q_e–q_t) versus time. The constants of the pseudo-first-order model, K_1 (h^{-1}), and the equilibrium capacity, q_e (mg/g), can be determined from the slope and intercept, respectively, based on the linear graph. Table 5 also contains these constants and the correlation coefficient R^2. The experimental data obtained for all three adsorbents used in the adsorption tests (the values in Section 3.4.1) did not correlate very closely with the plots. The highest correlation coefficient was found only for activated carbon. This confirms that the pseudo-first-order equation is not a suitable model for describing calcium adsorption kinetics using activated zeolite and alumina. Therefore, it is not logical to assume a linear driving force for the process of adsorption of calcium ions by zeolite and activated alumina used in this study, since the filling degree of adsorption sites is not proportional to the number of empty sites.

Table 5. Correlation coefficients and constant values of the kinetic models for the adsorption of calcium ions by different adsorbents.

Adsorbents	Pseudo-First Order			Pseudo-Second Order			Morris–Weber		
	R^2	q_e (mg.g^{-1})	K_1 (h^{-1})	R^2	q_e (mg.g^{-1})	K_2 (g mg^{-1}. h^{-1})	R^2	C (mg.g^{-1})	k_{id} (mg.g^{-1}. h$^{-0.5}$)
Zeolite clinoptilolite	0.9787	1.136	1.782	0.9978	3.868	4.951	0.9577	2.79	0.8833
Activated alumina	0.9776	0.531	2.422	0.9992	1.385	8.712	0.9138	0.7581	0.4772
Activated carbon	0.9938	0.51	3.652	0.9996	1.077	10.263	0.8654	0.6323	0.3264

3.5.2. Pseudo-Second-Order Kinetic Model

According to the pseudo-second-order kinetic model, the rate-limiting step may be a chemical adsorption reaction in which there is an electron exchange between the adsorbent and the adsorbate. Figure 19a–c show the linear plot of t/q_t as a function of time. The equilibrium capacities, q_e (mg/g), and the constant of the pseudo-second-order equation, k_2 (g/mg h), can be determined from the slope and the intercept of this plot, respectively. The calculated values of these constants and the correlation coefficients, R^2, are given in Table 5. According to these Figures, the experimental data for the three adsorbents used in the adsorption experiments fit well with the plots showing the desired correlation coefficient. Therefore, the pseudo-second-order equation can accurately describe the adsorption kinetics of calcium ions by adsorbents. According to this model, the degree of filling of adsorption sites is proportional to the square of the number of empty adsorption sites. The chemical reaction step is also one of the steps that control the adsorption of calcium ions by adsorbents.

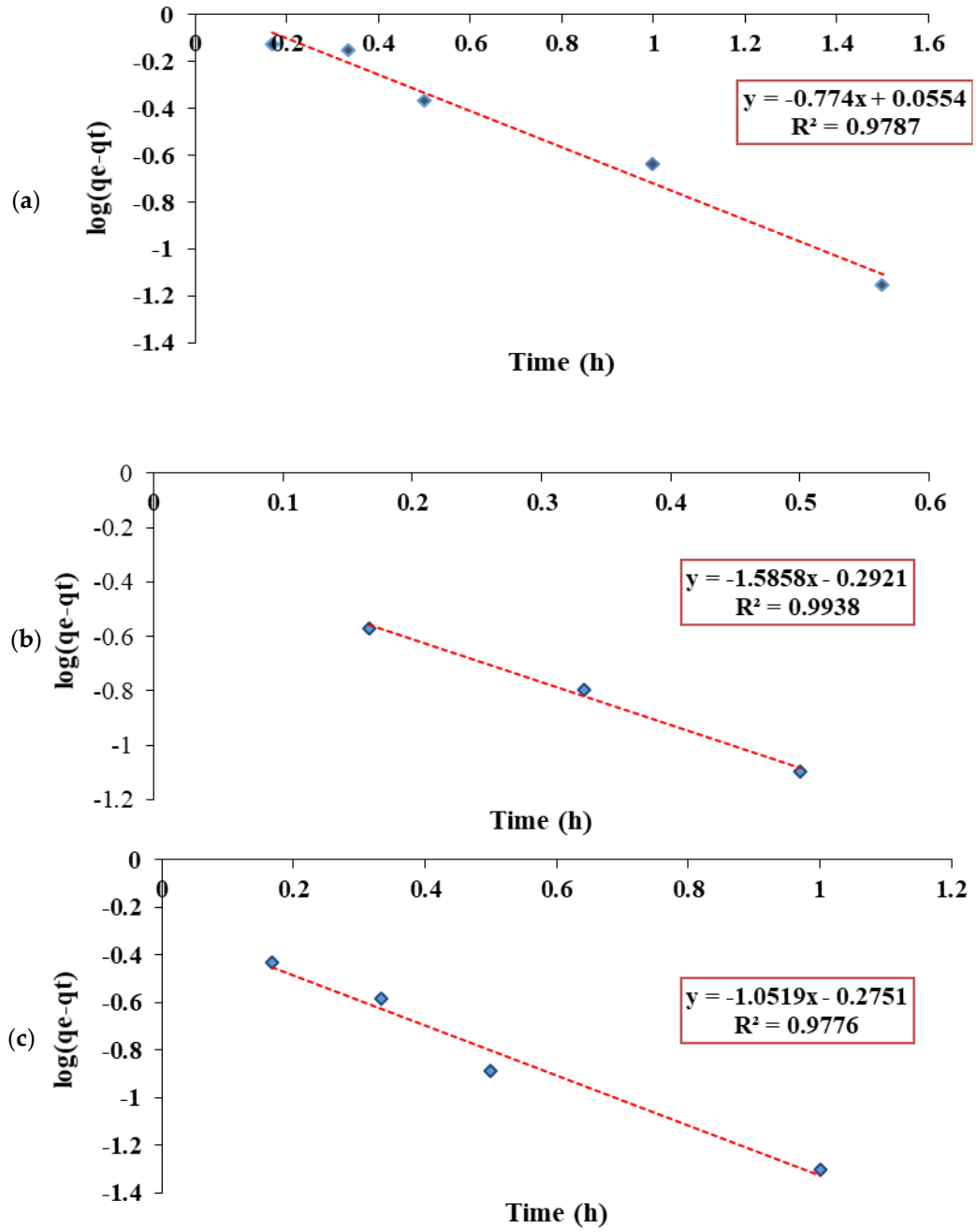

Figure 18. Linear plot of a pseudo-first-order kinetic model for the adsorption of calcium ions by (**a**) zeolite, (**b**) activated carbon, and (**c**) activated alumina.

3.5.3. Morris–Weber Kinetic Model

Figure 20a–c illustrate the plot of q_t versus time$^{0.5}$. If this plot is linear, the diffusion step can be assumed to control the adsorption process. In contrast, if this line passes through the origin of the plot, it can be argued that intraparticle diffusion is the only rate-limiting step. The constant values of the model, k_{id} (mg/G·h $^{0.5}$) and C (mg/g), can also be determined from the slope and intercept of q_t versus time$^{0.5}$. These calculated values and R^2 are summarized in Table 5. The experimental data obtained for all three adsorbents in the adsorption process are fitted with a relatively accurate correlation in the plots (Figure 20a–c). Due to the linearity of the graphs, it can be argued that intraparticle diffusion is one of the steps controlling the reaction rate of calcium ion adsorption by adsorbents. However, as the plot does not pass through the origin, intraparticle diffusion is not the only controlling factor for the reaction rate.

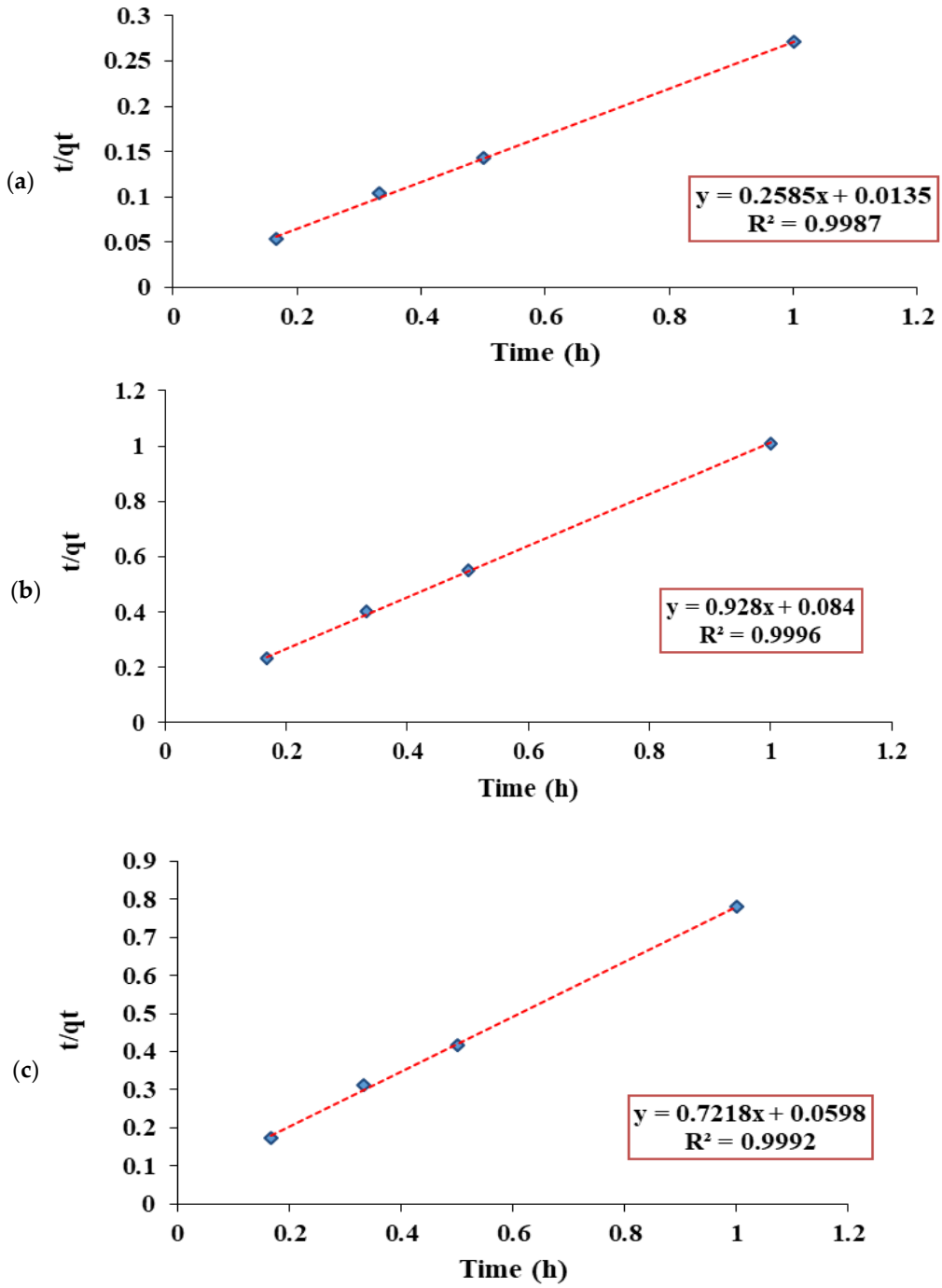

Figure 19. Linear plot of a pseudo-second-order kinetic model for the adsorption of calcium ions by (**a**) zeolite, (**b**) activated carbon, and (**c**) activated alumina.

Table 5 lists the calculated kinetic constants for the three adsorbents. Zeolite and activated carbon exhibit relatively high correlation coefficients compared to the other one, which is fitted with the linear plots of the adsorption kinetic models. Moreover, these adsorbents are fitted precisely with the pseudo-second-order equation. The rate-limiting step in this process is the chemical adsorption reaction involving electron exchange between the adsorbent and the adsorbate. In this context, it can be assumed that in the adsorption processes of the aqueous solution by the adsorbent, when there is a high concentration of the adsorbent in the aqueous solution, the pseudo-first-order equation prevails, while at low concentrations, the adsorption process fits the pseudo-second-order equation. The results for zeolite clinoptilolite also fitted relatively well with the Morris–Weber kinetic

model, confirming that intraparticle diffusion is another rate-limiting step in this reaction. Thus, the adsorption of calcium on adsorbents occurs in two stages, physical and chemical adsorption.

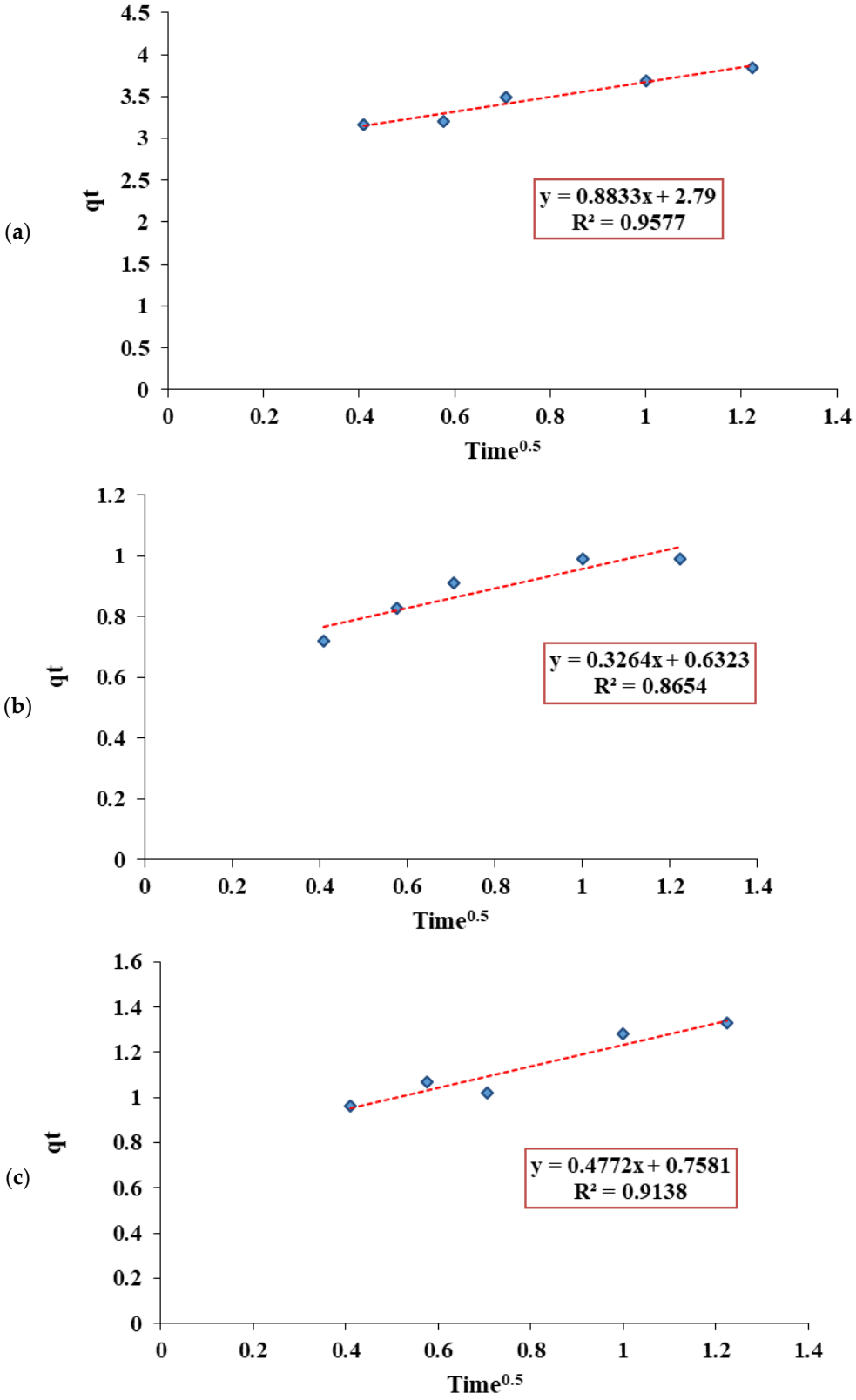

Figure 20. Morris–Weber kinetic model plot of calcium ion adsorption by (**a**) zeolite, (**b**) activated carbon, and (**c**) activated alumina.

4. Conclusions

In this study, the adsorption efficiency of hardness ions (calcium and magnesium) by different adsorbents (zeolite clinoptilolite, activated carbon, and activated alumina) and their modified forms with the same contact time were investigated. Our results show that increasing the adsorbent mass and contact time increased the hardness removal. The best concentrations of adsorbents used in the adsorption process of hardness ions (calcium and magnesium) for zeolite, carbon, and alumina were 40, 60, and 60 g/L in drinking water and 60, 40, and 40 g/L in groundwater, respectively. NaCl, HCl, and NaCl-HCl modifiers were used sequentially to improve the performance of the adsorbents. Salt-modified zeolite reduced the total hardness of the groundwater by 70.73%, while for the unmodified form, it was 59.23%. The acid modification resulted in the partial dissolution of alumina and zeolite and did not affect hardness removal. The highest hardness removal by activated carbon modified with acid and salt sequentially was 41.53% for drinking water. The pseudo-second-order kinetic model had the best fit to the experimental data. Moreover, the Langmuir model predicted the experimental data more accurately.

Author Contributions: Conceptualization, P.G., M.A. (Mohsen Abbasi), M.D. and M.A. (Mohammad Akrami); experimental tests, P.G., M.M.P. and M.J.D.; analysis of results, P.G., M.M.P. and M.A. (Mohsen Abbasi); visualization, M.J.D., A.R. and S.O.; supervision, M.A. (Mohsen Abbasi); writing of the manuscript, M.M.P.; writing—review and editing, M.M.P., S.O., M.D., A.R. and M.A. (Mohammad Akrami). All authors have read and agreed to the published version of the manuscript.

Funding: This research received no external funding.

Institutional Review Board Statement: Not applicable.

Informed Consent Statement: Not applicable.

Data Availability Statement: Not applicable.

Acknowledgments: The authors acknowledge Bushehr Water & WasteWater Company (Iran) for their financial support.

Conflicts of Interest: The authors declare no conflict of interest.

References

1. Nan Bakhsh, H. Chemical and microbial quality of drinking water sources. *Urmia Med. J.* **2003**, *11*, 41–50.
2. Amin, M.; Alazba, A.; Manzoor, U. A review of removal of pollutants from water/wastewater using different types of nanomaterials. *Adv. Mater. Sci. Eng.* **2014**, *2014*, 825910. [CrossRef]
3. Lall, S.P. The minerals. In *Fish Nutrition*; Elsevier: Amsterdam, The Netherlands, 2022; pp. 469–554.
4. Asghari, F.B.; Jaafari, J.; Yousefi, M.; Mohammadi, A.A.; Dehghanzadeh, R. Evaluation of water corrosion, scaling extent and heterotrophic plate count bacteria in asbestos and polyethylene pipes in drinking water distribution system. *Hum. Ecol. Risk Assess. Int. J.* **2018**, *24*, 1138–1149. [CrossRef]
5. Geldreich, E.E. *Microbial Quality of Water Supply in Distribution Systems*; CRC Press: Boca Raton, FL, USA, 2020.
6. Akram, S.; Rehman, F. Hardness in drinking-water, its sources, its effects on humans and its household treatment. *J. Chem. Appl.* **2018**, *4*, 1–4.
7. Emerson, A. *Quantitative Forecasting of Problems in Industrial Water Systems*; World Scientific: Singapore, 2003.
8. Shams, M.; Mohamadi, A.; Sajadi, S.A. Evaluation of corrosion and scaling potential of water in rural water supply distribution networks of Tabas, Iran. *World Appl. Sci. J.* **2012**, *17*, 1484–1489.
9. Świetlik, J.; Raczyk-Stanisławiak, U.; Piszora, P.; Nawrocki, J. Corrosion in drinking water pipes: The importance of green rusts. *Water Res.* **2012**, *46*, 1–10. [CrossRef]
10. Henthorne, L.; Boysen, B. State-of-the-art of reverse osmosis desalination pretreatment. *Desalination* **2015**, *356*, 129–139. [CrossRef]
11. Ping, Q.; Cohen, B.; Dosoretz, C.; He, Z. Long-term investigation of fouling of cation and anion exchange membranes in microbial desalination cells. *Desalination* **2013**, *325*, 48–55. [CrossRef]
12. Gowing, J. *Water and the Environment: Innovation Issues in Irrigation and Drainage*; CRC Press: Boca Raton, FL, USA, 2003.
13. Purkayastha, D.; Mishra, U.; Biswas, S. A comprehensive review on Cd (II) removal from aqueous solution. *J. Water Process Eng.* **2014**, *2*, 105–128. [CrossRef]
14. Goud, R.V.; Kumar, B.L.; Abhilash, N.; Prasad, P.R.; Saradhi, B.V. Comparision studies on adsorbants for removal of hardness from water by using newly prepared zeolite. *Int. J. Adv. Pharm. Biol. Chem.* **2015**, *4*, 342–354.

15. Pinto, X.; Al-Abed, S.R.; Balz, D.A.; Butler, B.A.; Landy, R.B.; Smith, S.J. Bench-scale and pilot-scale treatment technologies for the removal of total dissolved solids from coal mine water: A review. *Mine Water Environ.* **2016**, *35*, 94–112. [CrossRef]
16. Hamidpour, M.; Kalbasi, M.; Afyuni, M.; Shariatmadari, H.; Holm, P.E.; Hansen, H.C.B. Sorption hysteresis of Cd (II) and Pb (II) on natural zeolite and bentonite. *J. Hazard. Mater.* **2010**, *181*, 686–691. [CrossRef] [PubMed]
17. Yusof, A.M.; Malek, N.A.; Kamaruzaman, N.A.; Adil, M. Removal of Ca^{2+} and Zn^{2+} from aqueous solutions by zeolites NaP and KP. *Environ. Technol.* **2010**, *31*, 41–46. [CrossRef] [PubMed]
18. Bello, O.S.; Adegoke, K.A.; Olaniyan, A.A.; AbdulAzeez, H. Dye adsorption using biomass wastes and natural adsorbents: Overview and future prospects. *Desalination Water Treat.* **2015**, *53*, 1292–1315. [CrossRef]
19. Paul, P.J. *Value Added Products from Gasification Activated Carbon*; Combustion Gasifica-tion and Propulsion Laboratory Department of Aerospace Engineering; Indian Institute of Science: Bangalore, India, 2002.
20. Zsilák, Z.; Szabó-Bárdos, E.; Fónagy, O.; Horváth, O.; Horváth, K.; Hajós, P. Degradation of benzenesulfonate by heterogeneous photocatalysis combined with ozonation. *Catal. Today* **2014**, *230*, 55–60. [CrossRef]
21. Shokrolahzadeh, A.; Shokuhi Rad, A.; Adinehvand, J. Modification of nano Clinoptilolite Zeolite using sulfuric Acid and its application toward removal of Arsenic from water sample. *J. Nanoanalysis* **2017**, *4*, 48–58.
22. Mahvi, A.H.; Vosoughi, M.; Mohammadi, M.J.; Asadi, A.; Hashemzadeh, B.; Zahedi, A.; Pourfadakar, S. Sodium dodecyl sulfate modified-zeolite as a promising adsorbent for the removal of natural organic matter from aqueous environments. *Health Scope* **2016**, *5*, 1–8. [CrossRef]
23. Farrag, A.; Moghny, A.; Gad, A.M.; Saleem, S.S.; Fathy, M.; Ahmed, M. Removing of hardness salts from groundwater by thermogenic synthesis zeolite. *J. Hydrogeol. Hydrol. Eng.* **2016**, *5*, 9647.
24. Aghazadeh, S.; Safarzadeh, E.; Gharabaghi, M.; Irannajad, M. Modification of natural zeolite for Cu removal from waste waters. *Desalination Water Treat.* **2016**, *57*, 27843–27850. [CrossRef]
25. Akhtari, M.; Borazjani, H.; Arefkhani, M. Efficacy of lignocellulosics materials, zeolite and perlite for removal of cation and anions from sea and waste water. *Wood Res.* **2015**, *60*, 273–280.
26. Khatmode, N.P.; Thakare, S.B. Removal of pH, TDS, TSS & color from textile effluent by using sawdust as adsorbent. *Int. J. Sci. Basic Appl. Res.* **2015**, *24*, 158–163.
27. Rolence, C.; Machunda, R.; Njau, K.N. Water hardness removal by coconut shell activated carbon. *Proc. Int. For. Environ. Symp.* **2014**, *25*, 52. [CrossRef]
28. Sepehr, M.N.; Zarrabi, M.; Kazemian, H.; Amrane, A.; Yaghmaian, K.; Ghaffari, H.R. Removal of hardness agents, calcium and magnesium, by natural and alkaline modified pumice stones in single and binary systems. *Appl. Surf. Sci.* **2013**, *274*, 295–305. [CrossRef]
29. Payus, C.; Refdin, M.; Zahari, N.; Rimba, A.; Geetha, M.; Saroj, C.; Gasparatos, A.; Fukushi, K.; Oliver, P.A. Durian husk wastes as low-cost adsorbent for physical pollutants removal: Groundwater supply. *Mater. Today Proc.* **2021**, *42*, 80–87. [CrossRef]
30. Liu, W.; Singh, R.P.; Jothivel, S.; Fu, D. Evaluation of groundwater hardness removal using activated clinoptilolite. *Environ. Sci. Pollut. Res.* **2020**, *27*, 17541–17549. [CrossRef]
31. Mubarak, M.F.; Mohamed, A.M.G.; Keshawy, M.; Elmoghny, T.A.; Shehata, N. Adsorption of heavy metals and hardness ions from groundwater onto modified zeolite: Batch and column studies. *Alex. Eng. J.* **2022**, *61*, 4189–4207. [CrossRef]
32. Kaewmee, P.; Hungwe, D.; Takahashi, F. Adsorptive reduction of water hardness by a highly porous and regenerative geopolymer fabricated from coal fly ash waste with low-temperature calcination. *Environ. Sci. Pollut. Res.* **2021**, *28*, 54594–54607. [CrossRef]
33. Cai, P.; Zhao, J.; Zhang, X.; Zhang, T.; Yin, G.; Chen, S.; Dong, C.-L.; Huang, Y.-C.; Sun, Y.; Yang, D.; et al. Synergy between cobalt and nickel on $NiCo_2O_4$ nanosheets promotes peroxymonosulfate activation for efficient norfloxacin degradation. *Appl. Catal. B Environ.* **2022**, *306*, 121091. [CrossRef]
34. Zhang, R.; Li, D.; Sun, J.; Cui, Y.; Sun, Y. In Situ synthesis of FeS/Carbon fibers for the effective removal of Cr (VI) in aqueous solution. *Front. Environ. Sci. Eng.* **2020**, *14*, 1–12. [CrossRef]
35. Pourshadlou, S.; Mobasherpour, I.; Majidian, H.; Salahi, E.; Bidabadi, F.S.; Mei, C.-T.; Ebrahimi, M. Adsorption system for Mg2+ removal from aqueous solutions using bentonite/γ-alumina nanocomposite. *J. Colloid Interface Sci.* **2020**, *568*, 245–254. [CrossRef]
36. Gabol, N.M.; Khalique, A.; Memon, M.A.; Qureshi, A. Adsorption studies on the removal of cod and tds by using natural resources. *Int. Res. J. Mod. Eng. Technol. Sci.* **2021**, *3*, 1176–1180.
37. Zuo, Q.; Zhang, Y.; Zheng, H.; Zhang, P.; Yang, H.; Yu, J.; Tang, J.; Zheng, Y.; Mai, J. A facile method to modify activated carbon fibers for drinking water purification. *Chem. Eng. J.* **2019**, *365*, 175–182. [CrossRef]
38. Kumari, U.; Behera, S.K.; Meikap, B. A novel acid modified alumina adsorbent with enhanced defluoridation property: Kinetics, isotherm study and applicability on industrial wastewater. *J. Hazard. Mater.* **2019**, *365*, 868–882. [CrossRef] [PubMed]
39. Zereffa, E.A.; Bekalo, T.B. Clay Ceramic Filter for Water Treatment. *Mater. Sci. Appl. Chem.* **2017**, *34*, 69–74. [CrossRef]
40. Chambers, P. Standard methods for the examination of water and wastewater. *Sci. e-Resour.* **2019**, *21*, 130–170.
41. Omraei, M.; Najafpour, G.D. Removal of zinc from aqueous phase by charcoal ash. *World Appl. Sci. J.* **2011**, *13*, 331–340.
42. Asl, S.H.; Ahmadi, M.; Ghiasvand, M.; Tardast, A.; Katal, R. Artificial neural network (ANN) approach for modeling of Cr (VI) adsorption from aqueous solution by zeolite prepared from raw fly ash (ZFA). *J. Ind. Eng. Chem.* **2013**, *19*, 1044–1055. [CrossRef]
43. Tang, C.; Shu, Y.; Zhang, R.; Li, X.; Song, J.; Li, B.; Zhang, Y.; Ou, D. Comparison of the removal and adsorption mechanisms of cadmium and lead from aqueous solution by activated carbons prepared from Typha angustifolia and Salix matsudana. *RSC Adv.* **2017**, *7*, 16092–16103. [CrossRef]

44. Gupta, S.S.; Bhattacharyya, K.G. Immobilization of Pb (II), Cd (II) and Ni (II) ions on kaolinite and montmorillonite surfaces from aqueous medium. *J. Environ. Manag.* **2008**, *87*, 46–58. [CrossRef]
45. Katal, R.; Pahlavanzadeh, H. Zn (II) ion removal from aqueous solution by using a polyaniline composite. *J. Vinyl Addit. Technol.* **2011**, *17*, 138–145. [CrossRef]
46. Bhattacharya, A.K.; Naiya, T.K.; Mandal, S.N.; Das, S.K. Adsorption, kinetics and equilibrium studies on removal of Cr (VI) from aqueous solutions using different low-cost adsorbents. *Chem. Eng. J.* **2008**, *137*, 529–541. [CrossRef]
47. Horvath, G.; Kutics, K.; Suzuki, M. *Adsorption Engineering*; Kodansha: Tokyo, Japan, 1990; Volume 14.
48. Bansal, R.C.; Goyal, M. *Activated Carbon Adsorption*; CRC Press: Boca Raton, FL, USA, 2005.